U.PORTO
FEUP FACULDADE DE ENGENHARIA
UNIVERSIDADE DO PORTO

MECHANICAL INTERLOCK SYSTEM FOR REVERSIBLE PRECAST SLABS

RAPHAELA LOUISE DO NASCIMENTO FRANÇA

Dissertation submitted in partial fulfilment of the requirements for the degree of

MASTER IN CIVIL ENGINEERING STRUCTURES

Supervisor: Professor Dr. António Abel Henriques

Co-supervisor: Professor Dr. Agnese Scalbi

JUNE 2025

MASTER IN CIVIL ENGINEERING STRUCTURES 2024/2025

DEPARTMENT OF CIVIL ENGINEERING

Tel. +351-22-508 1901

✉ mestec@fe.up.pt

Edited by

FACULTY OF ENGINEERING OF THE UNIVERSITY OF PORTO

Rua Dr. Roberto Frias

4200-465 PORTO

Portugal

Tel. +351-22-508 1400

✉ feup@fe.up.pt

http://www.fe.up.pt

To my family.

"O sonho é ver as formas invisíveis
Da distância imprecisa, e, com sensíveis
Movimentos da esperança e da vontade,
Buscar na linha fria do horizonte
A árvore, a praia, a flor, a ave, a fonte
Os beijos merecidos da Verdade."

Fernando Pessoa

ACKNOWLEDGMENTS

As I reach the conclusion of this dissertation, I also bring to a close an important and transformative chapter of my life. I would like to express my deepest gratitude to everyone who has contributed, directly or indirectly, to making this work possible.

First and foremost, I thank my mother for her unwavering strength, constant support, and the values and faith she has instilled in me. Her love, even from afar, gave me the courage to face the most challenging moments.

To my husband, Bjarn, thank you for walking beside me with patience, generosity, and unconditional support. Your calm and gentle presence reminded me that it is possible to navigate life’s challenges with grace and affection.

I am deeply grateful to Professor Agnese Scalbi and Professor António Abel Henriques for their guidance, academic rigour, and generosity throughout this journey. Their insights, weekly meetings, and encouragement have been invaluable to the development of this research.

To my friends and colleagues, thank you for your companionship, honest conversations, and all the moments that made this journey lighter and more meaningful.

Finally, to everyone who supported me, even silently or without mention here, I offer my sincere thanks.

ABSTRACT

As sustainability and resource efficiency gain increasing prominence in the construction sector, there is a growing emphasis on design strategies that promote structural flexibility and circularity. Hollow core slabs, widely used in flooring systems, traditionally rely on cast-in-place mortar joints or concrete toppings to ensure composite behaviour. However, these conventional methods create permanent bonds that restrict the possibility of disassembly and reuse, thus limiting adherence to circular construction principles.

This research proposes an alternative demountable connection system based on mechanical interlocking steel connectors combined with localised reinforcement within the slabs. This solution facilitates efficient force transfer without the use of cast-in-place materials, enhancing demountability and enabling the recovery and reuse of structural components with minimal damage.

A prototype metallic connector is presented, featuring a total height of 126 mm. Its upper portion is cylindrical with a diameter of 100 mm, while the lower part tapers conically to 57 mm and includes openings that function as an interlock mechanism. The device is designed to engage with two 10 mm steel rebars embedded within the slabs, ensuring effective load transfer.

A finite element model was developed to simulate the behaviour of the slab system in a two-storey building subjected to horizontal wind loads. The simulations, performed using the ANSYS software package, evaluated the connector's strength, deformation under service and ultimate conditions, and its influence on the overall structural performance.

Preliminary results from the finite element analysis demonstrate that the steel connector combined with localised reinforcement can withstand the applied forces, supporting the feasibility of the proposed system to enable the reuse of hollow core slabs in circular construction.

KEYWORDS: Circular economy, Demountable connection, Design for disassembly, Hollow core slabs, Interlock mechanism.

RESUMO

À medida que a sustentabilidade e a eficiência no uso de recursos ganham relevância no sector da construção, cresce a procura por estratégias de projecto que promovam flexibilidade estrutural e circularidade. As lajes alveolares, amplamente utilizadas em sistemas de pavimentação, recorrem geralmente a juntas moldadas no local ou camadas de betão para garantir o comportamento composto. Contudo, essas soluções convencionais resultam numa ligação permanente entre os elementos, o que inviabiliza a desmontagem e reutilização das peças, comprometendo os princípios da construção circular.

Este trabalho propõe um sistema de ligação removível baseado em conectores metálicos de encaixe mecânico, associados a armaduras localizadas inseridas nas lajes. A solução permite uma transferência eficiente de esforços sem a utilização de materiais moldados in situ, favorecendo a desmontagem e a recuperação dos elementos estruturais com danos mínimos.

Apresenta-se um protótipo metálico com 126 mm de altura total. A parte superior possui formato cilíndrico com 100 mm de diâmetro, enquanto a parte inferior afunila em forma cónica até 57 mm e inclui aberturas que actuam como mecanismo de encaixe. O dispositivo é concebido para interagir com duas armaduras de aço de 10 mm posicionadas no interior das lajes, assegurando uma transferência eficaz de cargas.

Foi desenvolvido um modelo por elementos finitos para simular o comportamento do sistema de lajes num edifício de dois pisos sujeito à acção do vento horizontal. As simulações, realizadas com o software ANSYS, avaliaram a resistência do conector, as deformações em condições de serviço e de rotura, bem como o seu contributo para o desempenho estrutural global.

Os resultados preliminares da análise indicam que o conector metálico, em conjunto com a armadura localizada, suporta os esforços aplicados, confirmando a viabilidade do sistema proposto na reutilização de lajes alveolares em construções circulares.

PALAVRAS-CHAVE: Economia circular, Ligação desmontável, Projeto para desmontagem, Lajes alveolares, Mecanismo de encaixe.

LIST OF FIGURES

LIST OF TABLES

LIST OF SYMBOLS, ACRONYMS AND ABBREVIATIONS

Symbol	Description
α	Rotation factor (used for inclination analysis)
γ	Partial safety factor
Ψ	Combination factor
Ψt	Time-dependent combination factor
vb_0	Fundamental basic wind speed
vm	Mean wind speed
qp	Peak (extreme) wind pressure
cpe	External pressure coefficient
cpi	Internal pressure coefficient
Md;wind	Design bending moment due to wind
Vd;wind	Design shear force due to wind
kr	Terrain factor for roughness category
Iv	Turbulence intensity
Hi	Horizontal load due to inclination
l	Span length
E	Young's modulus
εcm	Strain at peak compressive strength
ψ	Dilatancy angle
fc2c	Biaxial compressive strength
Kcm	Plastic strain at peak compression

Acronym	Meaning
HCS	Hollow Core Slabs
FEM	Finite Element Method
DfD	Design for Disassembly
LI	Demountability Index
LIc	Connection Demountability Index
LIs	System Composition Demountability Index
DK	Crossing score (modularity parameter)
RO	Boundary condition score
TV	Type of connection score
ToV	Accessibility score
BIM	Building Information Modelling
ULS	Ultimate Limit State
SLS	Serviceability Limit State
RBD	Reversible Building Design
ISO	International Organization for Standardization
NS	Norwegian Standard
EN	European Norm (Eurocode)
TU/e	Eindhoven University of Technology

Abbreviation	Description
kN	Kilonewton
mm	Millimetre
m^2	Square metre
m^3	Cubic metre
°C	Degrees Celsius
MPa	Megapascal
kg	Kilogram
GPa	Gigapascal
%	Percent

1
INTRODUCTION

1.1. CONTEXT

Concrete is one of the most widely used building material. It is composed of cement, water and aggregates. While the formation of aggregates is a natural process with minimal carbon emissions, cement and water, which are the most used components in construction, are also the ones that most contribute to CO_2 emissions. In particular, the production of cement, which involves firing raw materials in a kiln, is responsible for up to 8% of global carbon emissions (Ramsden, 2020). At the same time, the construction sector generates the largest volume of waste within the European Union, largely due to demolition activities and the short lifespan of many building components.

To address these challenges, the reuse of structural concrete elements has emerged as a promising strategy to reduce both emissions and material waste. Reusing precast components can reduce the environmental footprint of construction processes significantly, with potential savings of up to 98% in embodied carbon and energy consumption during the production phase (ReCreate, 2022), when compared to the manufacturing of new precast elements. In response, the ReCreate project was launched to explore and improve the technical, economic, and systemic feasibility of reusing precast concrete elements at a structural level.

Among the various precast components available, hollow core slabs are particularly well suited for reuse. These prestressed elements are commonly used in residential and utility buildings due to their efficiency, reduced weight, and rapid installation. The slabs feature longitudinal voids that reduce material usage and dead load while maintaining structural performance. Compared to solid floor slabs, hollow core slabs enable longer spans and thinner sections, contributing to faster and more economical construction.

The slabs used in this study were produced by Consolis VBI and have a width of 1200 mm, a thickness of 260 mm, and a maximum span of 10 metres, as shown in Figure 1. Although hollow core slabs are standardised and modular, which enhances their reuse potential, their longitudinal joints are typically filled with cast in place mortar or concrete toppings. This traditional approach creates permanent bonds that restrict disassembly and complicate recovery.

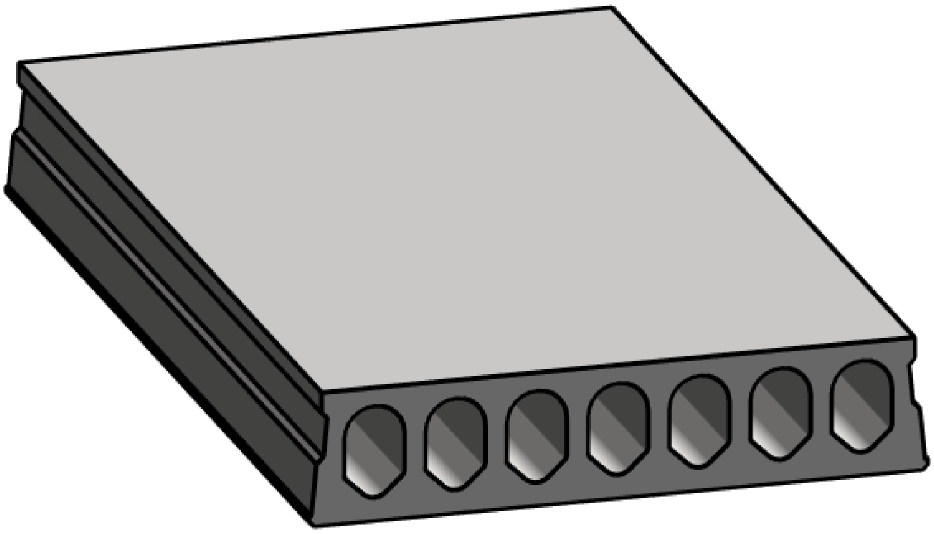

Fig. 1 - Geometry of the precast slabs used in this study (Consolis VBI).

Recent efforts, such as those by Lambrechts et al. (2024), have focused on creating demountable connection systems capable of restoring diaphragm action in reused hollow core slabs. Their work introduced a retrofit dowel-type connector as a solution for re-establishing continuity along modified slab edges following disassembly. While inspired by the same principles of reversibility and structural effectiveness, the present dissertation proposes a different approach by introducing a new connector geometry designed specifically to facilitate reuse without requiring bonded materials.

1.2. OBJECTIVES

This dissertation presents the development and evaluation of an innovative demountable connection system designed to enhance the circularity of precast concrete construction. The connector was created by the author as a response to the need for reversible slab systems capable of withstanding horizontal wind loads and achieving sufficient diaphragm action in precast floor assemblies.

The proposed solution consists of a mechanical interlock device made of steel, designed to work in combination with localised reinforcement embedded in the slabs. This configuration allows for the efficient transfer of forces across adjacent elements without the use of cast in place materials, thereby improving disassembly and enabling the recovery and reuse of components with minimal material degradation.

The connector prototype has a total height of 126 mm. Its upper section is cylindrical with a diameter of 100 mm, while the lower portion is conically shaped and tapers to a diameter of 57 mm. Openings in the lower part of the connector act as an interlock mechanism by anchoring the device to two 10 mm steel rebars placed within the slabs. This ensures effective transmission of forces and contributes to the structural performance of the slab system.

To assess its performance, a finite element model of a two-storey building with precast floor slabs was developed using ANSYS software. The model simulated the behaviour of the system under horizontal wind loads, with emphasis on the connector's contribution to the overall load transfer, deformation response, and serviceability under both service and ultimate limit states. Through this process, the mechanical interlock system was evaluated for its effectiveness in enabling reversible diaphragm action in a realistic building scenario.

1.3. RESEARCH QUESTIONS

Traditional connections between hollow core slabs, particularly those using cast in place mortar or structural toppings, pose a challenge for disassembly and reuse. These permanent joints hinder circular construction practices and highlight the need for alternative, demountable solutions. These methods create permanent bonds between elements, making it difficult to disassemble and repurpose the slabs without significant material damage. This restricts the application of circular construction principles and requires the development of alternative connection methods that are both structurally effective and reversible.

As outlined in the objectives, this research focuses on evaluating whether diaphragm action can be achieved in hollow core slab systems by applying interlocking steel connectors as a fully demountable solution. Specifically, the investigation examines the structural performance of these connectors in transferring shear loads generated by wind actions in a two-storey office building.

The central research question guiding this investigation is:

- Can diaphragm action be achieved using interlocking steel connectors as demountable joints in hollow core slab floors?

To answer this main question, the research is structured around the following sub-questions:

- What are the technical and practical criteria for a system to be considered demountable? (Addressed in Chapter 2.2. – Circular Construction and Design for Disassembly)

- What is the structural role of diaphragm floors within a building system, and how do they contribute to overall stability? (Addressed in Chapter 2.3.1. – Diaphragm Action in General)

- What are the performance requirements for joints in hollow core slabs to ensure diaphragm action, and which parameters most influence this behaviour? (Addressed in Chapter 2.3.2. – Diaphragm Action in Hollow Core Slabs)

- How does the proposed demountable connector behave structurally when subjected to longitudinal shear forces? (Explored in Chapter 5 – Discussion of Results)

- Can numerical simulations effectively represent the diaphragm behaviour of hollow core slabs connected by interlocking steel connectors? (Investigated in Chapter 4.3. – Numerical Modelling with ANSYS and Chapter 5 – Discussion of Results)

2
LITERATURE REVIEW

2.1. INTRODUCTION

This literature review begins by presenting a key study that served as the foundation and inspiration for this dissertation: Demountable Connection to Achieve Diaphragm Action by Lambrechts et al. (2024). Conducted within the framework of the European ReCreate Project, this research addresses critical challenges in the reuse of structural precast elements, particularly hollow core slabs (HCS), in the context of circular construction.

The Netherlands faces a dual challenge: meeting the urgent demand for approximately one million new homes by 2030, while simultaneously committing to a substantial reduction in carbon emissions with the goal of becoming carbon neutral by 2050. These goals are inherently conflicting under conventional construction practices. Lambrechts et al. propose that the reuse of structural elements offers a practical and sustainable path forward.

The study focuses on hollow core slabs, which are mass-produced, standardised elements widely used in floors of residential and office buildings. While HCS are well-suited for reuse due to their modularity, their longitudinal joints often filled with high-strength mortar or integrated with a cast-in-place topping pose significant challenges for disassembly. When these toppings are sawn off during demolition, the slabs lose their original interconnectivity, which compromises the diaphragm action required for lateral load resistance. This necessitates the development of new, demountable connection systems that can restore structural functionality without relying on bonded or permanent materials.

In response, the authors proposed a dowel-type connector, consisting of a metal pipe inserted into a cylindrical hole drilled at the joint between two adjacent slabs (Fig. 2). This dowel resists relative longitudinal displacement between the elements and aims to recover the in-plane shear transfer necessary for diaphragm action. The pipe has a standard outer diameter of 100 mm and is drilled to a depth of 100 mm ensuring it remains above the hollow voids within the slab cross-section. The connection is designed for ease of installation on-site, once the reused slabs are positioned, and is also adaptable in height depending on the presence of an in-situ topping layer.

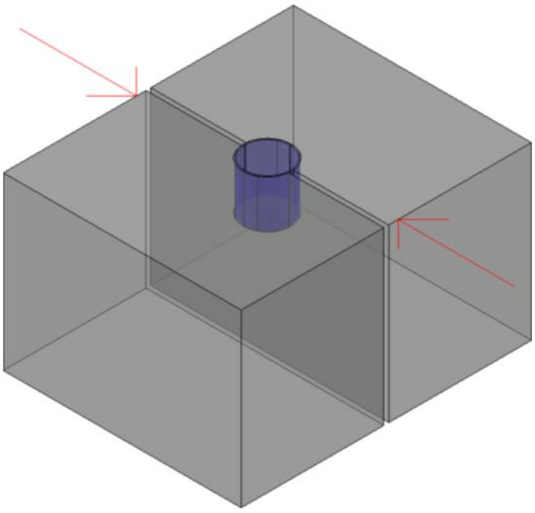

Fig. 2 - Conceptual sketch of the dowel-type connector inserted at mid-joint between adjacent HCS (Lambrechts et al., 2024)

Beyond shear transfer, the authors also consider the arching mechanism that develops in diaphragm systems under wind loads, where a horizontal tie is required to resist tensile forces (Fig. 3). The dowel system supports this action by ensuring a distributed lateral force path across the slab system. The authors suggest options for integrating these ties, such as using a continuous ring beam or direct slab-to-slab connections.

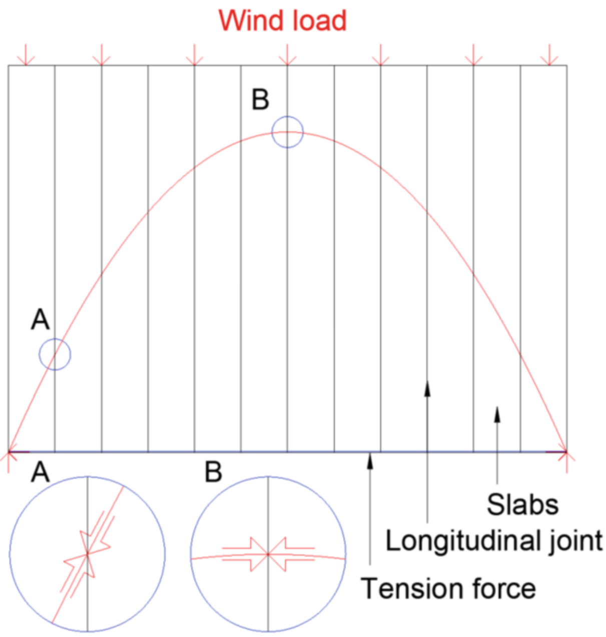

Fig. 3 - Illustration of the arching tie mechanism developed under horizontal wind load (Lambrechts et al., 2024)

To verify the connector's performance, finite element models (FEM) were developed. The first model evaluates force distribution in a slab field, examining how joint width and material stiffness influence the system's response. A second model analyses a single dowel embedded between slabs, considering variations in wall thickness, lateral compression, slab dimensions and eccentricities. The aim is to understand how these parameters affect both shear transfer and deformation, and ultimately how many dowels are required across a typical floor panel.

Complementing the FEM analysis, the study also outlines a detailed experimental setup (Fig. 4). It consists of a three-slab system: one full slab in the centre and two half-slabs on each side. Dowels are installed at specified intervals, and both longitudinal and lateral loads are applied using hydraulic pistons. The entire setup is self-contained, with forces balanced through internal tension rods rather than a fixed reaction floor. Displacements are measured with high-precision LVDTs, focusing on joint openings, dowel deformation and overall slab movement under load.

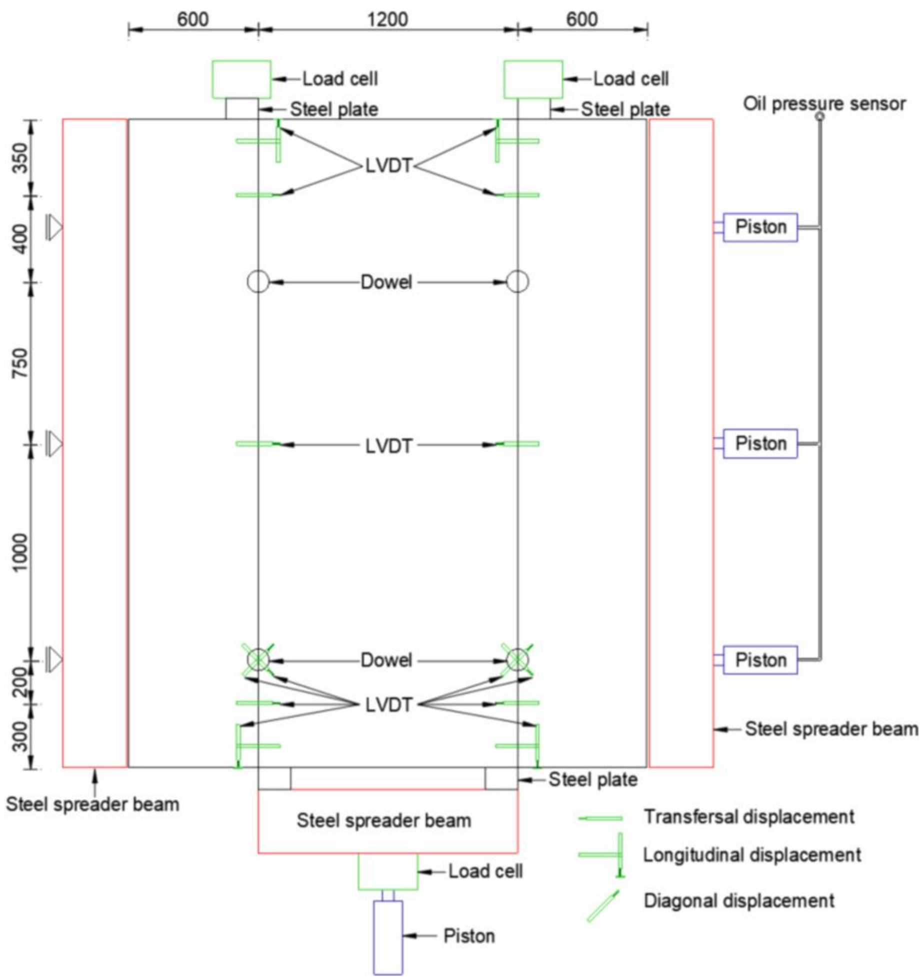

Fig. 4 - Laboratory test setup with central slab and two edge slabs connected via dowels (Lambrechts et al., 2024)

Early testing showed ductile failure modes in the dowel pipes, which is desirable as it allows the slabs themselves to remain undamaged and suitable for reuse. The authors performed a benchmarking test using aluminium pipes with 3 mm wall thickness, observing yielding at approximately 106 kN of force. Additional testing will explore different materials, wall thicknesses and even infilling the dowel with concrete to assess its influence on strength and stiffness.

The researchers emphasise that the dowel connector is intended for horizontal shear transfer only. It is not designed to carry vertical loads, which must still be addressed through bearing support or supplementary mechanisms in the structural layout.

Although the full results of the experimental campaign and FEM calibration were still under development at the time of publication, the Lambrechts study provides a thorough framework for understanding the requirements, constraints and opportunities in designing demountable connections for reused precast floors. This dissertation builds upon that foundation, proposing a new type of connector with a different geometry and load transfer strategy. While Lambrechts et al. opted for dowel resistance in a vertical hole, the present work explores the concept of mechanical interlock enhanced by embedded reinforcement, with the goal of achieving equivalent or superior diaphragm action in a fully reversible system.

Building upon the foundational study by Lambrechts et al., other key contributions in the field of circular construction and reusable precast systems provide further theoretical and technical grounding for this dissertation.

Durmisevic (2018), through the Reversible Building Design (RBD) framework, establishes core principles necessary for effective Design for Disassembly (DfD). The framework introduces three major pillars: (1) structural independence of primary load-bearing systems and secondary partitions, (2) dry, reversible connections, and (3) material and component traceability through systematic labelling or digital documentation. These principles are critical in ensuring that reused elements not only maintain their structural integrity, but also allow for future recovery and reconfiguration.

In particular, the second pillar dry and reversible connections has direct relevance to this research. Conventional cast-in-place (CIP) methods are incompatible with DfD principles because they result in permanent joints that must be destroyed for disassembly. Conversely, a mechanical connector that can be inserted and removed without altering the host elements aligns closely with RBD. The proposed mechanical interlock connector was conceived with these principles in mind, especially in how it engages rebars mechanically without the use of adhesives or chemical bonding.

Another essential reference is the Demountability Index proposed by van Vliet et al. (2021). This index quantifies a structure’s disassembly potential based on several weighted criteria, including: (1) type of connection (e.g. dry, bonded, welded), (2) accessibility, (3) dependency on surrounding components, and (4) removability without damage. Dry, accessible, and independent connectors receive the highest ratings. In applying this system, the proposed connector would likely achieve a high demountability score due to its non-invasive installation, ease of access, and minimal reliance on adjacent components.

Van Vliet et al. (2021) further note that the reuse of structural components is often inhibited not only by technical barriers, but also by logistical and informational limitations such as lack of documentation, unclear structural history, or inability to identify embedded reinforcements. Their study reinforces the need for design strategies that include both physical reversibility and lifecycle transparency. The connector proposed in this dissertation attempts to address both fronts: mechanically, by avoiding bonded materials, and operationally, by allowing traceability through simple detailing and exposed access.

Additionally, existing standards and technical guidelines provide a regulatory backdrop that both supports and limits innovation in reusable construction. EN 1168+A3 (2011) defines performance requirements for hollow core slabs, including shear key dimensions and guidelines for diaphragm behaviour. However, it does not explicitly accommodate reuse scenarios or demountable joints. Annex D of the standard specifies how slabs should transfer in-plane forces across joints, typically via structural toppings or grouted shear keys both of which are incompatible with disassembly.

To fill this regulatory gap, the Norwegian standard NS 3682 (2022) was introduced to guide the reuse of hollow core slabs. It includes dismantling procedures, load-bearing assessments, and structural verification methods tailored to reused elements. The standard emphasises pre-demolition documentation and the need for reliable testing protocols. While not legally binding outside Norway, NS 3682 serves as a valuable model for other national guidelines. It recognises that reused slabs may not fit neatly into factory-production parameters and proposes verification through testing, labelling, and on-site validation.

Moreover, ISO 20887 (2020) formalises the concept of DfD within an international context, offering both conceptual definitions and practical design strategies. It advocates for independent joining systems, simplicity in design, and avoidance of adhesives or finishes that hinder reuse. These guidelines align strongly with the design philosophy of the present work. The connector system developed here avoids any form of wet or destructive connection, reinforcing ISO's vision of adaptable, reusable construction.

2.2. CIRCULAR CONSTRUCTION AND DESIGN FOR DISASSEMBLY

Circular construction aims to extend the service life of building components while reducing waste and environmental impact throughout the lifecycle of a structure. It moves away from the traditional linear model of “take, make, dispose” by promoting reuse, recycling, and adaptability. Within this framework, structural components are designed not only for performance but also for future recovery and reconfiguration.

Within the context associated to the circular construction concept of Design for Disassembly (DfD), the demountability of components becomes a measurable design goal. The work of Veenhuis (2024) provides a detailed methodology for quantifying the demountability of structural systems using a Demountability Index (LI). This index is calculated from two sub-indices: the connection demountability index (LIc), and the composition demountability index (LIs). Each of these is itself derived from specific technical parameters:

- LIc is based on the type of connection (TV) and its accessibility (ToV). TV scores range from 0.1 (chemical or irreversible joints) to 1.0 (dry mechanical joints), while ToV scores reflect whether the connection can be accessed and removed without damage.
- LIs evaluates the degree of modularity (crossing score, DK) and the boundary conditions for disassembly (RO), again scored from 0.1 to 1.0 depending on the level of integration and the ease of removal.

These indices are combined via the equations:

LIc = (2/3 × TV) + (1/3 × ToV)

LIs = (2/3 × DK) + (1/3 × RO)

And finally:

LI = (2/3 × LIc) + (1/3 × LIs)

This system allows comparison between products and assemblies in terms of how easily and cleanly they can be disassembled. In practice, it has been used in sustainability tools, product certification, and digital material passports. For example, dry mechanical connectors like the one proposed in this dissertation typically score highly in both TV and ToV, making them favourable in life-cycle assessments and circular design evaluations.

Barriers to reuse have also been emphasised in studies such as Veenhuis (2024), which notes that traditional joint systems using high-strength mortar or monolithic toppings not only prevent reversibility but often require destructive techniques like sawing. This alters the original geometry of the slabs, making reuse difficult or impossible in many cases. The present research addresses this by offering a fully reversible connector that avoids permanent alterations to the slabs and enhances the LI score of the structural system.

CUR recommendation (1990) complements this view by defining demountability as the ability to remove structural elements without unacceptable damage or environmental disruption. This reinforces the importance of dry, mechanical, and independent joints that preserve both structural integrity and geometric compatibility for future use.

Finally, embracing DfD also requires addressing structural interaction. Elements must perform together under load even if they are designed for disassembly. The proposed connector aims to satisfy this balance by ensuring effective diaphragm action through interlocking engagement, thus meeting both structural and circularity demands.

In summary, this section has highlighted the conceptual and quantitative frameworks that inform the development of demountable systems. By following DfD principles and optimising for high LI values, the connector developed in this dissertation contributes meaningfully to the broader goals of circular construction.

2.3. DIAPHRAGM ACTION

2.3.1. DIAPHRAGM ACTION IN GENERAL

Diaphragm action is a fundamental mechanism in structural engineering that enables floor or roof systems to transfer horizontal loads, such as those from wind or seismic events to the vertical structural elements of a building. By functioning as horizontal beams, diaphragms distribute lateral forces to shear walls or moment-resisting frames, contributing significantly to the global stability of the structure and preventing excessive deformation or collapse.

For diaphragm action to be effective, the floor system must exhibit adequate in-plane stiffness and shear strength. These properties are essential to resist racking deformations and torsional effects, while ensuring a uniform distribution of internal forces. The ability of a diaphragm to fulfil this role depends on several key factors, including: the continuity and rigidity of the slab system, the quality and configuration of connectors or joints, and the boundary conditions at the slab's supports.

Diaphragms are typically classified as rigid, semi-rigid, or flexible, based on how they deform in relation to the lateral force-resisting system. Rigid diaphragms assume uniform deformation across their surface and distribute loads proportionally to the stiffness of supporting elements. Flexible diaphragms, on the other hand, distribute loads based on tributary area, often leading to increased displacements and non-uniform behaviour. Semi-rigid diaphragms exhibit characteristics between these two extremes. In precast concrete structures, particularly those lacking monolithic toppings, achieving diaphragm action is more complex and often demands mechanical or bonded connections across slab joints.

In multi-storey buildings, the presence of an effective diaphragm is vital for controlling interstorey drift, redistributing lateral loads, and managing torsional irregularities caused by asymmetrical layouts or stiffness imbalances. Without such a system, localised damage or instability can propagate, particularly under dynamic loading conditions.

An arch pattern of compressive stresses develops in the slab and is accompanied by tension forces in the horizontal ties or chords, as illustrated in Figure 5 (Soeprapto et al., 2016). These components are essential to form the force-resisting mechanism of the diaphragm.

Fig. 5 - Development of forces in a diaphragm (Joostdevree, 2024)

To function properly, a diaphragm must include the following key elements:

- Chords or tension ties that resist axial tension or compression, forming the upper and lower flanges of the diaphragm "beam."
- A diaphragm web that resists in-plane shear forces, often composed of the main body of the floor slab.
- Collectors or drag struts that transfer lateral forces from the diaphragm web into the chords, ensuring continuity of force flow.

These components are schematically illustrated in Figure 6, where a top view of a floor shows the interrelation between web, chords, and collectors (Buettner & Becker, 1998).

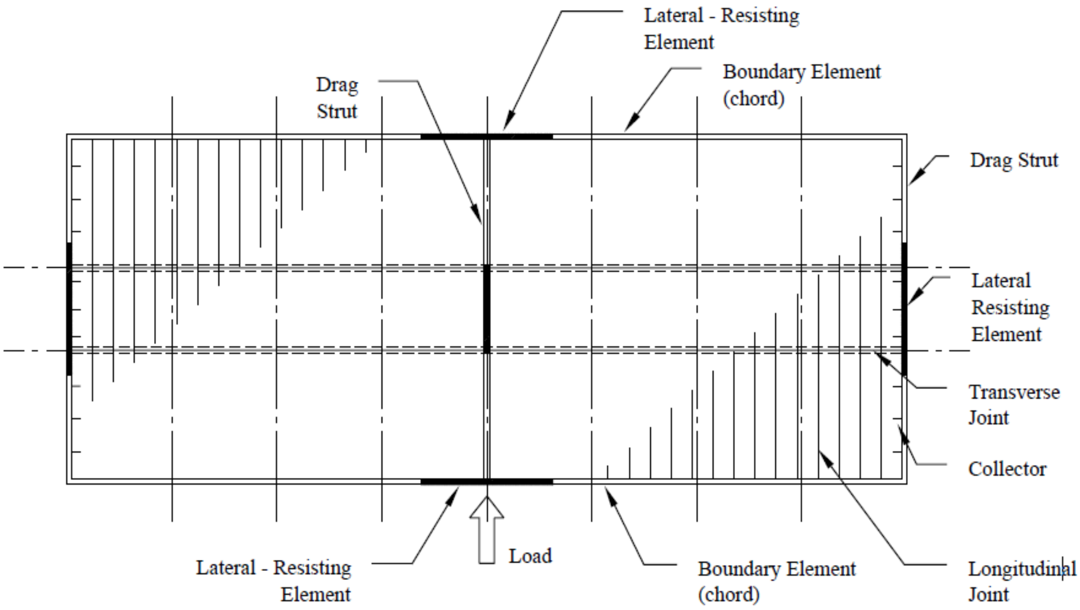

Fig. 6 - Top view of a floor, with a schematisation of the elements of a diaphragm (Buettner & Becker, 1998)

Understanding these principles is crucial for evaluating new connection systems in precast floors, particularly when aiming to restore or replicate diaphragm action in reused elements. The effectiveness of such systems is not limited to their shear capacity but also involves their integration into a holistic load path that ensures compatibility with structural performance requirements under service and ultimate limit states.

2.3.2. DIAPHRAGM ACTION IN HOLLOW CORE SLABS

Hollow core slabs (HCS) are precast, prestressed elements widely used in floor systems due to their reduced weight, high structural efficiency, and modular design. Despite these advantages, individual HCS units cannot function as diaphragms on their own, as they are not continuous in the horizontal plane. Ensuring diaphragm action in HCS systems requires the effective transfer of in-plane shear forces between adjacent slabs.

The most common solution is the application of a cast-in-place reinforced concrete topping, which fills the longitudinal keyways and creates a rigid, monolithic surface. When properly designed and constructed, such toppings enable the slabs to act as a composite diaphragm, distributing lateral loads across the floor system. A topping of at least 50 mm is typically required to ensure sufficient shear transfer and global stiffness.

However, the inclusion of a structural topping introduces constraints. It increases material use, extends construction time and, most critically, creates permanent bonds that hinder future disassembly. This directly opposes circular construction strategies where reversibility and reusability are essential.

In topping-free systems, the capacity of the floor to act as a diaphragm depends entirely on the ability of the longitudinal joints to transfer shear. Traditional solutions often involve grouting these joints with cementitious materials. While this may provide temporary stiffness, long-term performance is limited. Studies have shown that such joints are prone to degradation, cracking and water ingress, compromising both durability and safety.

As a result, there is growing interest in dry mechanical alternatives capable of ensuring reliable shear transfer without the use of bonded materials. These solutions must not only provide adequate structural performance but also support modularity and ease of disassembly, particularly for reuse scenarios.

Understanding the challenges and mechanisms of shear transfer in hollow core slab joints is fundamental when evaluating or developing new connection systems. The performance of these joints directly affects the stability and serviceability of the overall structure, especially under horizontal actions such as wind or seismic loading.

3
DESIGN TO WIND LOADS

3.1. INTRODUCTION

To establish a realistic and technically sound basis for evaluating the structural performance of the proposed demountable connector, a set of wind load calculations was carried out. These calculations were grounded in a representative case study involving a hypothetical two-storey office building situated in a suburban region of the Netherlands. The aim of this exercise was to simulate the type and magnitude of horizontal actions that floor systems in such structures would typically be subjected to during their service life, particularly under wind loading conditions.

By assessing the distribution and intensity of wind-induced pressures acting on the building envelope, it was possible to derive the corresponding horizontal forces transmitted through the structural diaphragm at each floor level. These forces are critical for determining the internal shear demands acting across the longitudinal joints between adjacent hollow core slabs, which are the locations where the proposed connector is expected to ensure effective load transfer.

The analysis was conducted in strict accordance with the provisions outlined in Eurocode 1, Part 1-4 (EN 1991-1-4), which governs the determination of wind actions on structures across Europe. This standard provides a rigorous framework for calculating wind pressures based on factors such as building geometry, exposure category, basic wind speed, terrain roughness and pressure coefficients for various structural surfaces. Adhering to these guidelines ensures that the derived load values are both consistent with accepted engineering practice and applicable to a wide range of practical design scenarios.

By grounding the assessment in a realistic structural context and adhering to established codes, this approach offers a reliable reference point for evaluating whether the proposed connector can effectively transfer shear forces under wind loading. This is an essential consideration in the validation of its structural viability within diaphragm floor systems.

3.2. WIND LOAD CALCULATION

3.2.1. BUILDING GEOMETRY AND SITE CONDITIONS

To estimate the stresses occurring in the floor diaphragm, it is first necessary to determine the distribution of forces within it. The horizontal wind load induces bending moments, shear forces, and normal forces in the plane of the floor. By estimating the magnitude of these forces, it is possible to approximate the loads that the connectors will need to withstand.

To assess the load-bearing capacity of the connectors, a hypothetical scenario was considered to estimate the applied forces, providing a basis for evaluating their structural performance.

This calculation applies to an office building with the following dimensions, see Figure 7.

L × B = 30 m × 15 m
H = 3 × 3,20 m = 9,60 m

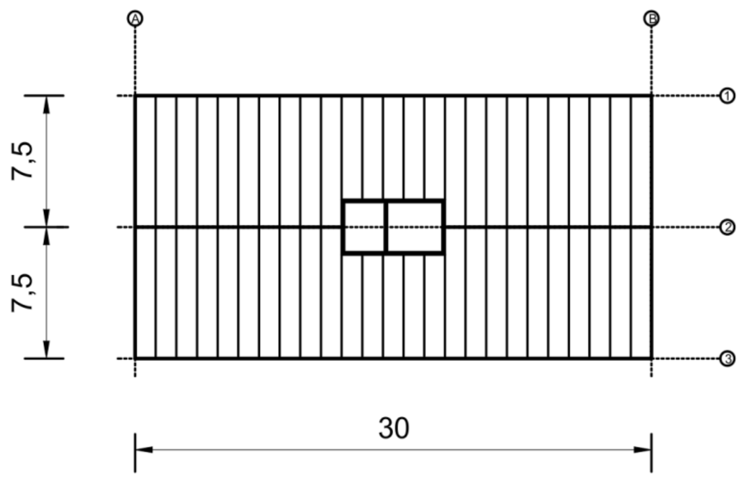

Fig. 7 - Geometry of the case study building.

3.2.2. MATERIAL PROPERTIES AND SAFETY FACTORS

The roof and floor slabs are prefabricated hollow-core slabs, supported by edge and intermediate beams. The span of the slabs is 7,50 m

The stability of the building is ensured by the concrete core walls and the diaphragm action of the floor slabs.

For the structural assessment, the following conditions apply:

- Safety class: 2
- Reference period: 50 years
- Reduction factor: $\Psi = 0$, thus $\Psi t = 1$
- Considered area: Area 2

For the Ultimate Limit State (ULS), the load factors are:

- Permanent favorable load: $\gamma = 0{,}9$
- Permanent unfavorable load: $\gamma = 1{,}2$
- Variable load: $\gamma = 1{,}5$

For the Serviceability Limit State (SLS), all γ-factors are equal to 1.

The floor system consists of VBI hollow-core slab elements.

The main characteristics of the slabs are as follows:

- Manufacturer: VBI
- Slab width: 1200 mm
- Slab thickness: 260 mm
- Weight per square meter: 383 kg/m² (3,76 kN/m²)
- Characteristic raw material: Concrete C45/55.

3.2.3 LOADS CALCULATIONS

<u>Roof Floor:</u>

- Permanent Load
  HCS 260 mm: 3,76 kN/m²
  Insulation, pipes: 0,35 kN/m²
  Total Permanent Load: 4,11 kN/m²
- Variable Load
  Office load (people and equipment): 1,00 kN/m²

<u>Floor:</u>

- Permanent Load
  HCS 260 mm: 3,76 kN/m²
  Insulation, pipes, finishing floor: 1,15 kN/m²
  Non-structural internal walls: 0,50 kN/m²
  Total Permanent Load: 5,41 kN/m²
- Variable Load
  Office load (people, furniture, furnishings): 2,50 kN/m²

3.2.4. DETERMINATION OF WIND LOAD

Wind area		II	
Fundamental Basic Wind speed	vb0	27,0 [m/s]	

EN-1991-1-4 (Dutch version)

Section 4.3.2 Terrain Roughness

Height above ground level		z	9,6 [m]	
Roughness length		z0	0,05 [m]	*Terrain Category II*
Terrain factor for category II		z0II	0,05 [m]	
Terrain factor	$k_r = 0{,}19 \cdot \left(\frac{z_0}{z_{0,II}}\right)^{0{,}07}$	kr	0,19 [-]	
Roughness factor	$c_r(z) = k_r \cdot \ln\left(\frac{z}{z_0}\right)$	cr	0,9989 [-]	

Section 4.3.1 Variation with Height

Orography factor		co	1 [-]	*Recommended in 4.3*
Base wind speed for wind area 2		vb,0	27,0 [m/s]	
Mean wind speed	$v_m(z) = c_r(z) \cdot c_o(z) \cdot v_b$	vm	26,9649 [m/s]	

Section 4.4 Wind Turbulence

Turbulence factor	kl	1 [-]
Turbulence intensity	Iv	0,1902

Section 4.5 Extreme Wind Pressure

Extreme wind pressure qp 1,06 [kN/m²]

$$q_p(z) = (1 + 7\, I_v(z)) \cdot ½ \cdot \rho \cdot v_m^2(z) = c_e(z) \cdot q_b$$

Section 7.2 Pressure coefficients for buildings

Wind perpendicular to longitudinal facade

External pressure coefficient cpe 0,8 [-]

μ = 0,6875 [-]

Internal pressure coefficient cpi 0,10 [-]

Table 1 - Recommended values of external pressure coefficients for vertical walls of rectangular plan buildings (EN 1991-1-4: Eurocode 1 – Actions on structures – Part 1-4: General actions – Wind actions, Table 7.1.)

Zone	A		B		C		D		E	
h/d	$c_{pe,10}$	$c_{pe,1}$	$c_{pe,10}$	$c_{pe,1}$	$c_{pe,10}$	$c_{pe,1}$	$c_{pe,10}$	$c_{pe,1}$	$c_{pe,10}$	$c_{pe,1}$
5	-1,2	-1,4	-0,8	-1,1	-0,5		+0,8	+1,0	-0,7	
1	-1,2	-1,4	-0,8	-1,1	-0,5		+0,8	+1,0	-0,5	
≤ 0,25	-1,2	-1,4	-0,8	-1,1	-0,5		+0,7	+1,0	-0,3	

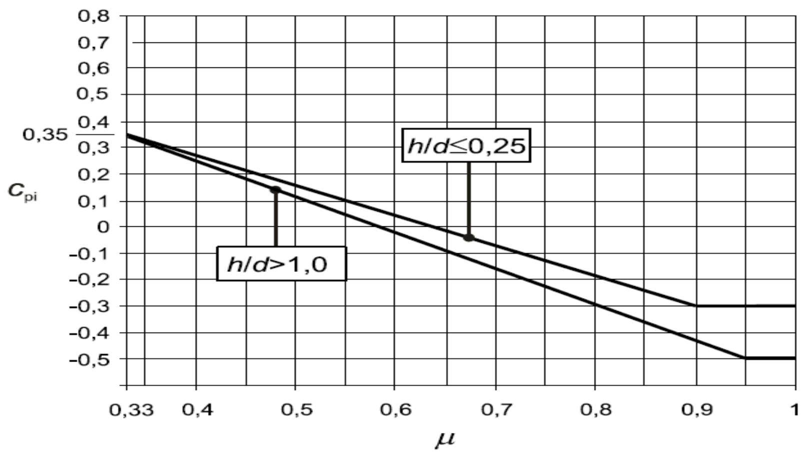

Fig. 8 - Internal pressure coefficient for uniformly distributed openings (EN 1991-1-4: Eurocode 1 – Actions on structures – Part 1-4: General actions – Wind actions, Figure 7.13)

Wind Force on longitudinal facade:

Fw = (Cpe + Cpi) x qp(z) = (0,80 + 0,10) x 1,06 = 0,954 kN/m²

The floor slabs are modelled as a beam supported at two points, with a span of 30 meters. The calculation follows the standard method for tension tie reinforcement.

Determination of the load on a standard intermediate floor due to wind:

Wind pressure line load:

q-load due to wind pressure = 1,5 (γ) × 0,954 × 3,2 (floor height) = 4,58 kN/m

Determination of the load on the first floor due to inclination (first order analysis), see Figure 9.

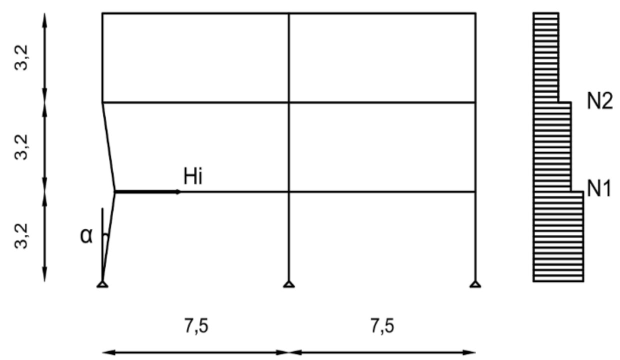

Fig. 9 - Inclination (first order analysis)

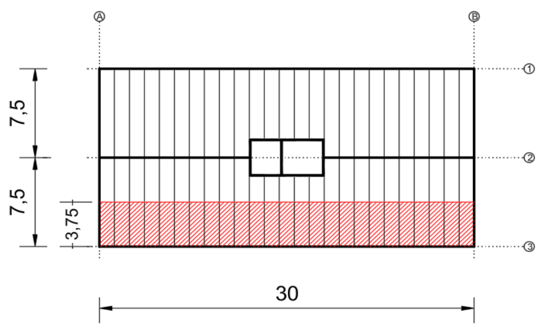

Fig. 10 - Area for determining skewness

$H_i = \alpha \times (N1 + N2)$

N1	= 3,75 × [(1,2 × 5,41 + 1,5 × 2,50) + (1,2 × 4,11 + 1,5 × 1,00)]	= 62,53 kN/m
Self-weight of walls	0,15 × 20,55 × 3,2 × 2	= 19,73 kN/m
		= 82,26 kN/m

N2	= 3,75 × (1,2 × 4,11 + 1,5 × 1,00)	= 24,12 kN/m
Self-weight of walls	0,15 × 20,55 × 3,2	= 9,86 kN/m
		= 33,98 kN/m

A value of 0.002 (1/500) is used for the factor α.

$H_i = 0{,}002 \times (82{,}26 + 33{,}98) = 0{,}23$ kN/m

Determination of Bending Moment on the Beam

$M_{d;wind} = (1/8) \times q_{d;beam} \times l^2$

$M_{d;wind} = (1/8) \times (4{,}58 + 0{,}23) \times 30^2 = 541$ kNm

Determination of Shear Force on the Beam

$V_{d;wind} = (1/2) \times q_{d;beam} \times l$

$V_{d;wind} = (1/2) \times (4{,}58 + 0{,}23) \times 30 = 72{,}2$ kN

Based on the wind pressure distribution on the building envelope, the total horizontal force acting on each floor was estimated using standard assumptions regarding load transfer. With a tributary height of 3.2 metres per storey and a building width of 9.6 metres, the distributed wind load was applied across the slab span to evaluate the internal forces generated in the floor system.

In the most critical case under wind loading, the bending moment acting on the floor diaphragm was found to be approximately 541 kNm. The corresponding design shear force acting along the span reached 72.2 kN. This shear force represents the load that must be transferred across the longitudinal joints between adjacent hollow core slabs to maintain diaphragm action and ensure horizontal load continuity.

These values define the service-level demands that the proposed connector must withstand. In particular, the estimated shear force of 72.2 kN per joint serves as a key reference for the structural modelling and performance evaluation presented in the next chapters.

4

CONNECTOR DESIGN AND OPERABILITY EVALUATION

4.1. CONNECTOR DESIGN

The development of the connector proposed in this dissertation began with a detailed investigation of the hollow core slabs selected for analysis. The initial step consisted of identifying a commonly used slab type in the European precast industry, in contrast with the relatively less conventional slabs studied by Lambrechts et al. (2024). Through the VBI (Consolis) website, one of the leading manufacturers of precast concrete elements in the Netherlands, the Revit file of a widely adopted 260 mm thick hollow core slab with a width of 1200 mm was obtained. This allowed for a precise understanding of the internal and external geometry of the slab, including its reinforcement layout and the physical profile of the longitudinal joints.

Upon analysing the slab geometry provided in the BIM model, it became evident that the edges of the joints were different from those studied by Lambrechts et al. (2024). In their research, the reused slabs featured straight, cut edges resulting from demolition, which provided clean surfaces for the installation of cylindrical dowels. In contrast, the slabs used in this dissertation have a factory-defined interlocking profile in the longitudinal joints, typical of prestressed hollow core slabs produced under controlled conditions. This variation in joint geometry played a crucial role in shaping the design approach of the connector.

The choice to work with VBI slabs was not only based on their geometric definition but also on their prevalence in actual construction practice. These slabs are widely used in residential and commercial projects across Europe, making them a highly relevant candidate for reuse strategies. The aim of this research was to propose a connector that could be realistically applied in common structural systems, thereby improving the chances of practical adoption within circular construction workflows.

While Lambrechts et al. (2024) proposed a dowel-type connector specifically designed to resist horizontal shear between adjacent slabs, they explicitly stated that the system was not intended to carry vertical loads. Vertical shear transfer, in their case, had to be provided by additional bearing supports or structural toppings. This limitation presents a challenge when considering scenarios where localised loads, such as a point or line load applied to a single slab, must be redistributed through diaphragm action to adjacent slabs.

With that motivation in mind, this dissertation explores the possibility of a connector that does more than resist horizontal shear. The goal was to create a system capable of also engaging in vertical shear transfer between slabs, enabling full participation in the diaphragm mechanism even in the absence of cast-in-place toppings. This condition becomes particularly relevant in configurations where differential loading is applied to a single slab unit, and redistribution through inter-slab shear becomes necessary. An example of such a scenario is illustrated in Figure 11, where a uniformly distributed line load is applied along one slab, creating the need for horizontal and vertical force transmission through the joint to maintain structural equilibrium.

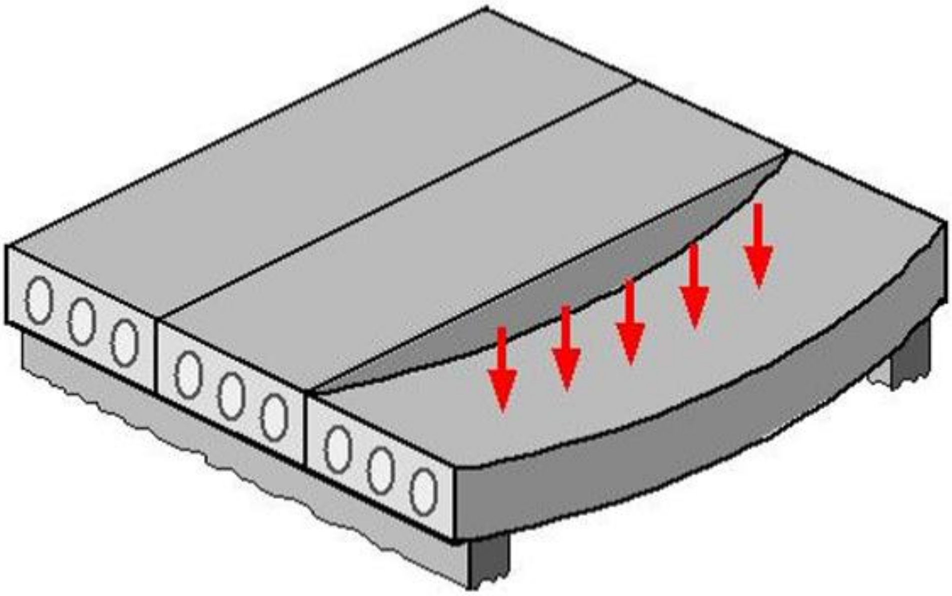

Fig. 11 - Example of a single hollow core slab subjected to a distributed line load parallel to the span (EN 1168)

To achieve vertical shear transfer, it was necessary to integrate steel reinforcement (rebars) embedded within the slabs into the connector system. This presented a technical challenge: how to ensure effective and reversible anchorage between the connector and the rebars, without relying on bonded materials. The solution was found in the concept of mechanical interlock.

The connector was designed in two parts. The upper section is cylindrical, sized to match the pre-drilled circular void between the slabs and to make direct contact with the concrete. The lower section is conical and fits the internal profile of the joint. This tapered base contains internal slots positioned to receive the embedded reinforcing bars.

Four alternative geometries were created and assessed during development. The version shown in Figure 12, a standalone 3D model of the connector with the rebars, was selected because it delivers reliable interlock and is straightforward to install on site. The sequence is simple: the reinforcing bars are first inserted into the slab voids; the connector is then placed vertically and rotated 90°, so that the slots engage the bars and lock the slabs together.

After this rotation, the bars are held firmly, creating a mechanical bond that prevents vertical and horizontal movement between adjacent slabs. The mechanism maximises contact surface and resists both tensile and compressive forces without any cast-in-place material, providing a dry, reversible connection stiff enough to maintain diaphragm action.

Several iterations were refined in Revit, adjusting slot alignment, fabrication tolerances and installation clearances in conjunction with the slab profile. The final arrangement, integrated between two hollow-core slabs, is illustrated in Figure 13, confirming compatibility with the internal voids and joint geometry.

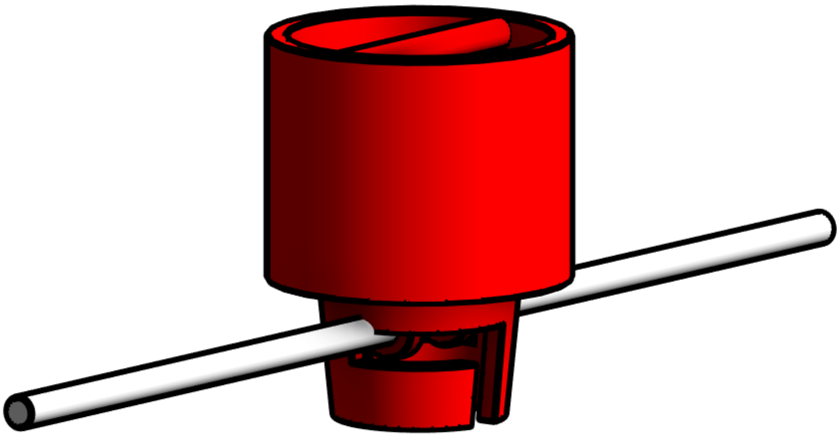

Fig. 12 - 3D model of the connector with the rebars.

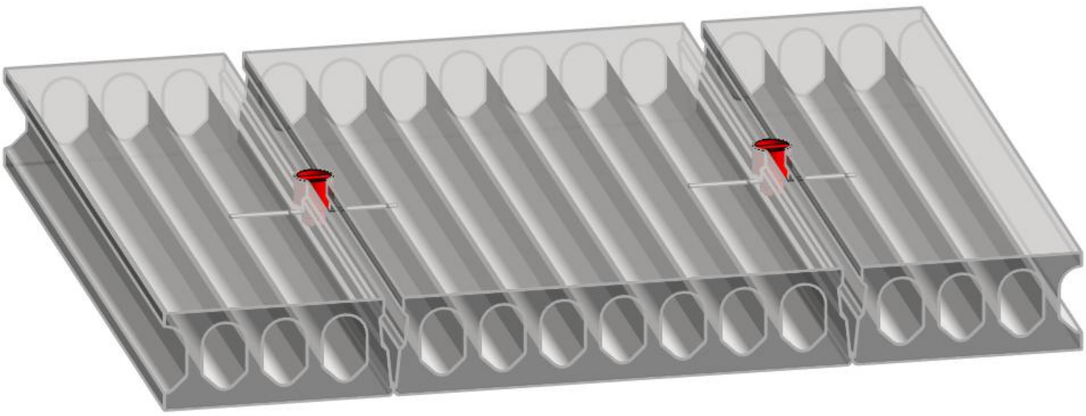

Fig. 13 - 3D representation in Revit showing the final connector geometry aligned with the internal joint profile of the hollow core slabs.

By aligning the connector's geometry with the existing slab joint profile and integrating a mechanical anchorage solution through the use of rebars, the design balances structural performance with the principles of demountability. This lays the foundation for the operability testing presented in the following section.

4.2. OPERABILITY TEST

4.2.1. Materials and Methods

To assess the operability of the mechanical connector for reversible precast slab systems, a series of physical tests were conducted using a full-scale timber prototype. The objective was to simulate realistic assembly conditions and evaluate how the connector interacts with different rebar end configurations within the interlock system, identifying which option performs most effectively.

4.2.2. Timber Prototype Configuration

A solid timber block measuring 240 × 240 mm was used to simulate a cross-section of two precast concrete slabs. The block was cut into two equal halves, each representing one of the slabs to be connected. A machined slot in the centre of the block allowed for the insertion of the metallic connector, produced at TU/e. This connector acted as the central component of the interlock mechanism.

In each half-block, aligned holes were drilled to allow the insertion of rebars through the connector. The setup enabled repeated and adjustable testing of various rebar configurations while allowing for clear visual inspection and manual handling.

Fig. 14 - Timber block.

Fig. 15 - Timber prototype.

Fig. 16 – Connector

4.2.3. Rebar end Detail Configurations

Test 1: Straight Rebar (Simple End) + Simple Connector

A standard straight-ended bar was inserted through the connector. The main issue observed was that the rebar could slide inside the connector opening, compromising the stability of the interlock.

Pros:
• Fast and simple insertion
Cons:
• Prone to sliding inside the connector
• Lacked mechanical resistance to longitudinal movement

Fig. 17 - Straight rebar + timber block.

Fig. 18 - Interlock System 1.

Test 2: Straight Rebar + Connector with Slot

To address the sliding issue observed in Test 1, a semicircular slot (5 mm radius) was made in the conical portion of the connector, where the interlock mechanism is located, as shown in the figure below.

Pros:
• Successfully blocked rebar movement
• Provided a passive mechanical locking

Cons:
• Does not prevent lateral movement, so the interlock mechanism may not block side-to-side displacement
• Requires accurate positioning of the rebar

Fig. 19 - Connector with slots.

Fig. 20 - Interlock System 2.

Test 3: Upward-Bent Rebar + Connector with Slot

A rebar with an upward bend at its end was tested with the connector that has the slot. However, considering that rebar is placed in the slab before the slabs are aligned and the cylindrical hole is drilled into them, the available length for the bent segment becomes minimal. This makes fabrication more difficult, as the bend would require high precision over a very short segment.

Pros:
• Prevented pull-out and slippage
• Provided mechanical anchorage without modifying the connector interior

Cons:
• Required precise rebar fabrication and rotation during assembly
• Short length of bent end made production difficult

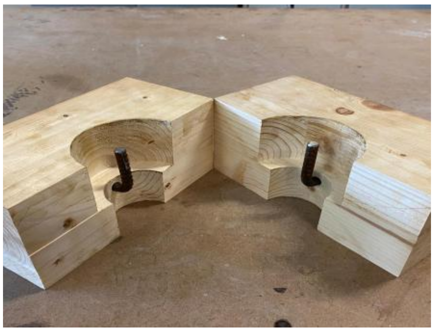

Fig. 21 - Upward-bent rebar + timber block.

Fig. 22 - Interlock System 3.

Test 4: Downward-Bent Rebar + Connector with Slot

A rebar with a downward-facing bent end was tested using the same connector that had a slot. This configuration provided a longer bent segment, which simplified the bending process and improved manufacturability. However, if the bent end was not strictly oriented downwards, the insertion of the connector could become more difficult, as misalignment might hinder the proper passage of the rebars through the connector's openings.

Pros:
• Provided good mechanical lock against movement
• Enabled a longer bent end segment

Cons:
• Installation more difficult if the bent part is misaligned
• Potential interference during assembly

Fig. 23 - Downward-bent rebar + timber block.

Fig. 24 - Interlock System 4.

Test 5: Rebar with Welded Metal Cap ("Nail Head") + Connector with Slot

In this configuration, a 10 mm screw with a scroll head was used to simulate a rebar with a small circular metal plate welded to its end, creating a nail head that effectively blocked movement. This was the best-performing configuration, as it prevented both sliding and large lateral displacements of the rebar within the connector.

Pros:
• Prevented rebar sliding and large lateral movements
• Provided a highly reliable mechanical stop

Cons:
• Required welding, increasing fabrication effort

Fig. 25 - Welded metal cap rebar + timber block.

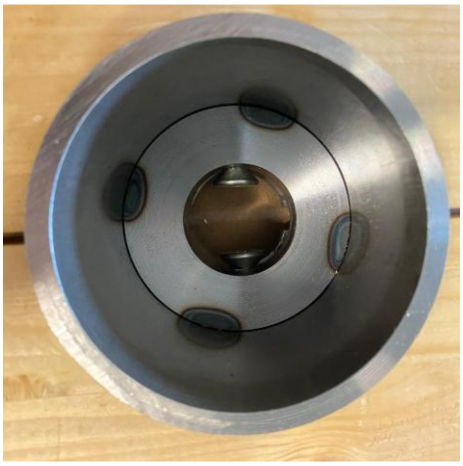

Fig. 26 - Interlock System 5.

Fig. 27 - Proposed rebar configuration with welded "nail head" plate.

4.2.4. Conclusion

The operability tests conducted using the timber prototype provided valuable insights into the performance of the mechanical connector under various rebar end configurations. The initial test with a straight rebar highlighted the need for additional locking mechanisms, as the bar tended to slide freely within the connector. The addition of a semicircular slot in the conical portion of the connector proved effective in preventing longitudinal movement, although it did not address lateral displacements.

Bent rebar configurations introduced new considerations. The upward-bent rebar offered good anchorage but required a short and precisely fabricated bent segment, which complicates production. The downward-bent configuration, on the other hand, allowed for a longer bent segment, easing fabrication. However, its success depended heavily on correct orientation during installation, or it could interfere with the connector placement.

Among all tested configurations, the solution involving a welded metal cap ("nail head") at the rebar end demonstrated the best overall performance. It reliably prevented both longitudinal and lateral movements, ensuring secure engagement within the connector. Despite the additional fabrication effort due to welding, this configuration offers a robust and efficient solution for use in reversible precast slab systems, combining simplicity of application with mechanical effectiveness.

Additionally, a small steel bar was applied at the top of the connector to assist with its rotation during installation. This feature improved the practical handling of the connector.

Fig. 28 - Final Connector Design

4.3. NUMERICAL MODELLING WITH ANSYS

4.3.1. PURPOSE AND CONTEXT OF THE SIMULATION

To complement the manual calculations and operability tests described in earlier sections, a numerical investigation was performed using the finite element software ANSYS. The goal of this simulation was to provide a deeper understanding of the structural behaviour of the proposed demountable connector under realistic loading conditions. The focus was particularly on its ability to transfer in-plane shear forces between precast hollow core slabs without the use of cast-in-place materials.

The modelling aimed to reproduce a setup representative of laboratory testing conditions, allowing for the observation of load transfer mechanisms, interface behaviour, stress development, and potential failure modes. In doing so, it provides valuable insights into the connector's effectiveness within a diaphragm system, supporting its feasibility for circular construction practices.

4.3.2. FINITE ELEMENT MODELLING SETUP AND SIMULATION PROCEDURE

The finite element model was based on the same configuration envisioned for experimental validation in the laboratory, as illustrated in Figure 29. This physical test setup consists of three hollow core slab segments mounted within a rigid steel frame to ensure structural alignment and effective force application. The central slab, representing a full-width precast element, has dimensions of 1200 mm width × 2000 mm length × 260 mm height, while the adjoining slabs are 600 mm wide half-units. The applied load configuration includes a vertical load (F) distributed through two contact points on the central slab, while reaction forces (Rn) are transmitted through supports beneath the half slabs. A prestressing force (P) is also applied longitudinally along the two outer slabs to mimic realistic in-service conditions.

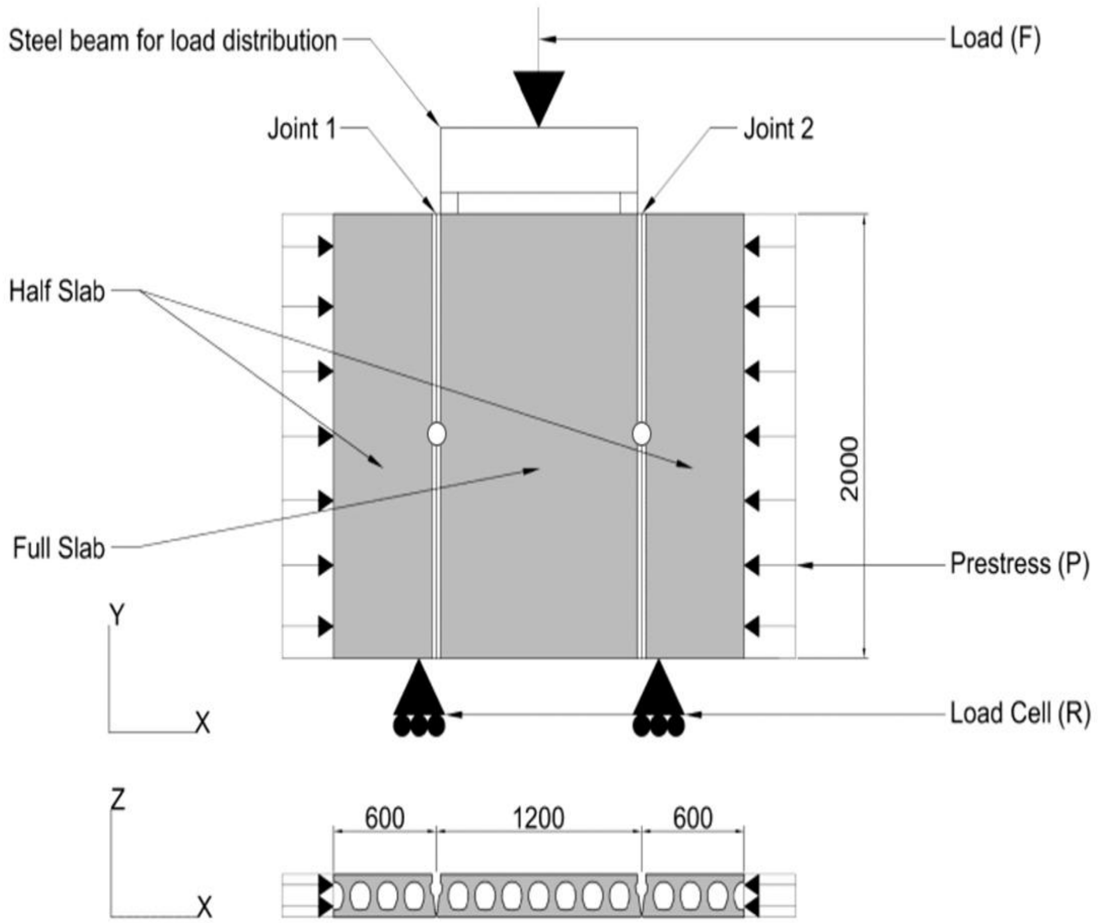

Fig. 29 - Schematic representation of the experimental test setup used as the basis for the numerical modelling.

To accurately replicate the geometry of the hollow core slabs and ensure integration with the connector system, the geometry was imported directly from a BIM model in Revit. This guaranteed that the internal voids, slab cross-section, and joint details were modelled according to industry standards as illustrated in Figure 30 and Figure 31.

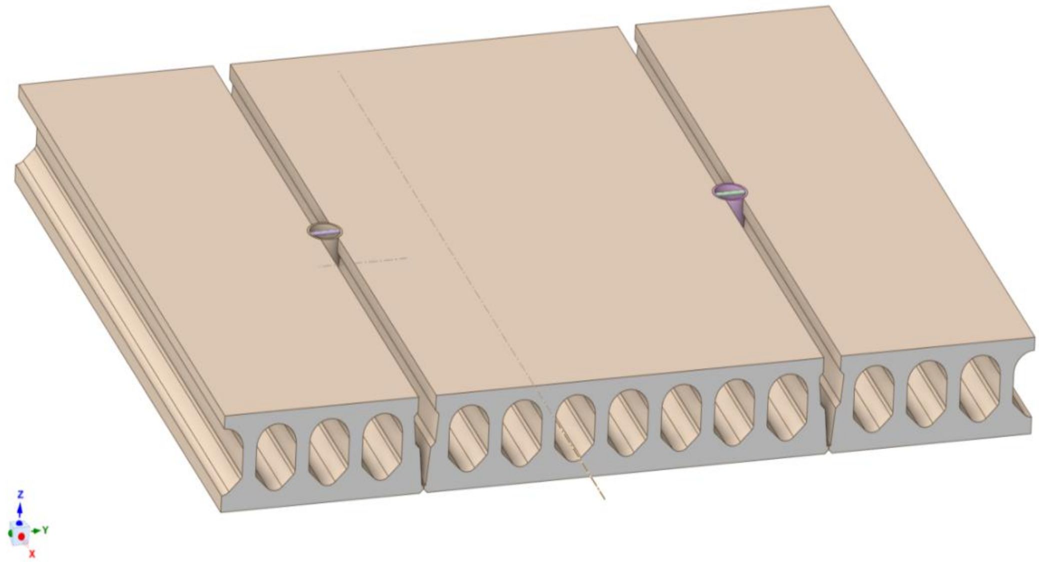

Fig. 30 - Overall finite element model geometry showing the full assembly of hollow core slabs and connector integration.

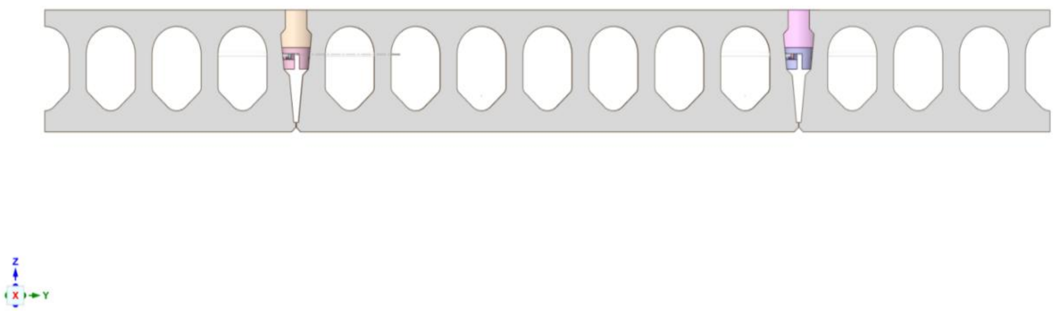

Fig. 31 - Section view of the finite element model highlighting internal voids and joint detailing in the slab-to-slab connection.

Concrete was modelled using nonlinear material behaviour consistent with C45/55 properties, including:

- Young’s Modulus: 36 GPa
- Poisson’s Ratio: 0.20
- Modulus of Rupture: 4.9 MPa
- Biaxial Compressive Strength (fc2c): 52 Mpa (per fib MC 2010 Section 5.1.6 comentary)
- Dilatancy Angle (ψ): 30° (assumed)
- Strain at Peak Compression (εcm): 0.0024 (per fib Model Code 2010 Table 5.1-8)
- Plastic Strain at Peak Compression (Kcm): 0.001

To capture the post-peak and residual behaviour of concrete, additional parameters were defined for both compressive and tensile responses. These were crucial for ensuring model stability and for replicating energy dissipation mechanisms during cracking and crushing:

- Ultimate Plastic Strain in Compression: 0.01
- Relative Stress at Nonlinear Hardening: 0.4
- Residual Compressive Relative Stress: 0.2
- Plastic Strain Limit in Tension: 0.01
- Residual Tensile Relative Stress: 0.2

These material parameters were selected based on existing literature and international design codes, then calibrated through preliminary simulations to avoid divergence and to enhance the convergence of the solver in nonlinear conditions.

Steel (Connector and Rebars): Elastic-perfectly plastic material with a yield strength of 500 MPa. This defines the stress threshold beyond which plastic deformation occurs without additional increase in load.

No strain hardening was included in the steel model to maintain simplicity and avoid additional computational effort, as this was not expected to significantly affect the overall behaviour in the context of diaphragm action.

Element Types and Contact Modelling

The geometry was discretised using the following finite elements:

- Solid185 Elements: Applied to the concrete domains, these elements allow for the inclusion of nonlinear material properties and large deformations.

- Beam188 Elements: Used for representing the embedded reinforcement and the metallic connector, suitable for slender structural components under combined loading.

Contact elements were incorporated to define the interaction between the concrete slabs and the connector. Depending on the loading condition, the contact was defined as either bonded (no relative motion) or frictional (allowing slip), to capture various stages of force transfer across the joint.

Mesh Configuration

A structured mesh was adopted in order to improve the quality and reliability of the finite element solution. The mesh characteristics were as follows:

- Concrete Domains: Meshed using hexahedral elements (Solid185), which provide better accuracy in stress prediction, particularly in three-dimensional stress states.

- Steel Components: Modelled with line elements (Beam188) to minimise computational cost while maintaining structural accuracy.

- Mesh Density: The mesh was refined around the connection regions to capture localised stress concentrations. The final element size was defined as 40 mm, balancing accuracy and computational efficiency.

The finalised finite element mesh is presented in Figures 32 and 33, offering both a global and detailed representation of the numerical model. Figure 32 displays the complete mesh of the structural system, encompassing the hollow core slabs and the integrated connector. This comprehensive view is fundamental for understanding the spatial distribution of elements and the interaction among the main components. In contrast, Figure 33 provides a detailed view of the mesh in the vicinity of the connector and the reinforcement bars, focusing on the critical zones where load transfer and stress concentrations are expected to occur.

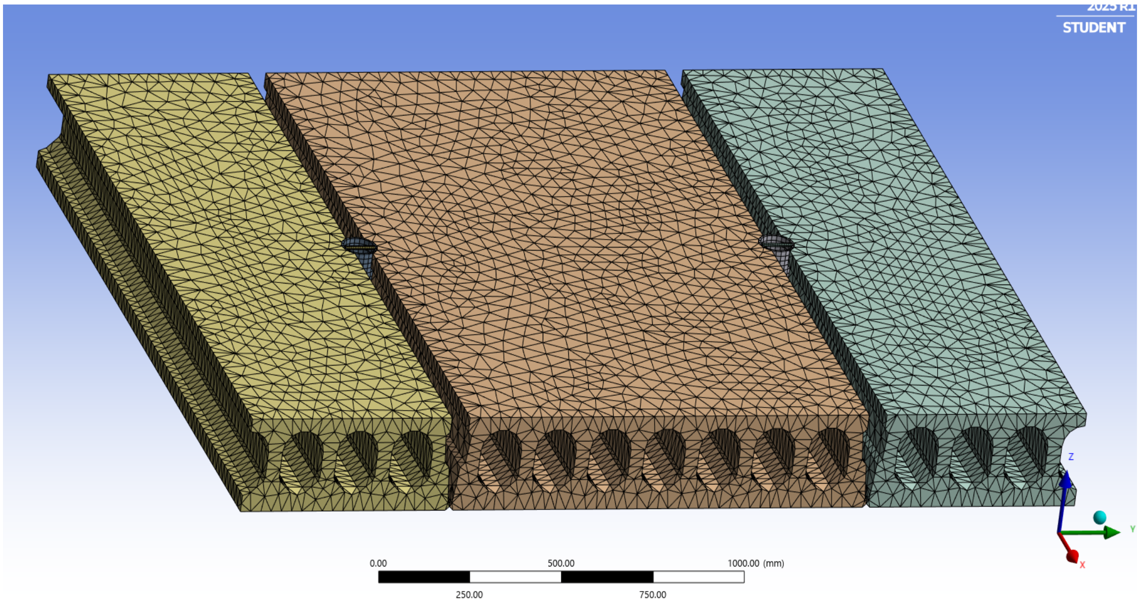

Fig. 32 - Finite element mesh generated in ANSYS showing the complete structural assembly, including hollow core slabs and connector integration.

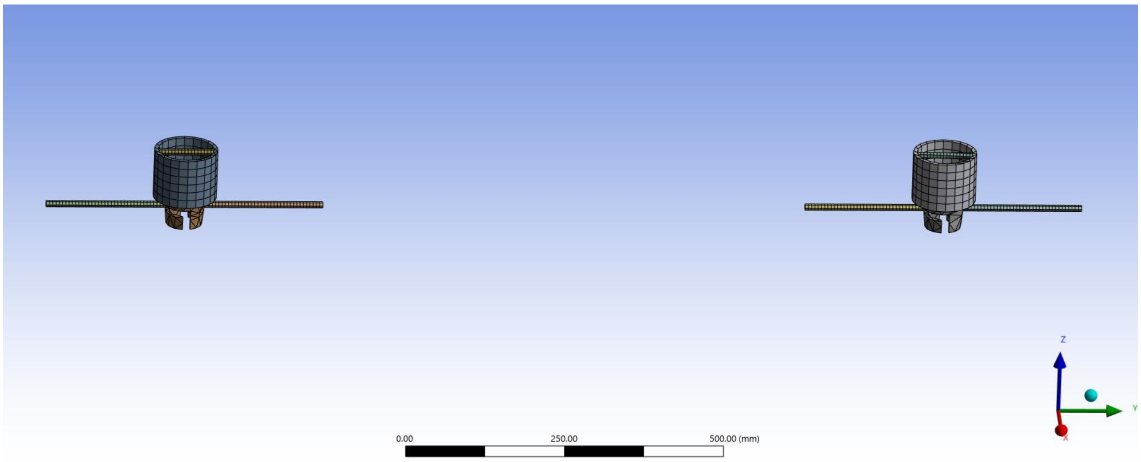

Fig. 33 - Detailed view of the finite element mesh around the connectors and reinforcement rebars.

The model was developed to simulate a scenario representing a worst-case condition for shear transfer between precast slabs. The boundary conditions and loading were defined as follows:

- Boundary Restraints:
  The two outer slabs were fully restrained in all translational and rotational degrees of freedom, simulating the support rig in a test setting.

- Loading Condition:
  A horizontal displacement of 1 mm was imposed on the central slab, simulating the effects of lateral loading (e.g., from wind or seismic action) and forcing the system to mobilise the connector for shear transfer.

- Prestressing Simulation:
  Although prestressing strands were not modelled explicitly, their effect was introduced as initial stress conditions along the reinforcement in the outer slabs.

This displacement-controlled loading strategy was chosen instead of a force-based or pressure-based approach in order to improve control over the nonlinear solution and to simulate deformation-based behaviour typical of in-situ conditions.

The developed finite element model enabled a detailed assessment of the connector's structural performance under imposed horizontal displacement. It effectively captured the interaction between the connector, concrete, and reinforcement components, while also illustrating the stress distribution and deformation patterns throughout the system. The simulation provided valuable insights into several key aspects, including:

- Identification of local stress concentrations around the connector region;

- Evaluation of shear force transfer mechanisms through the mechanical interlock system;

- Assessment of global stiffness and the capacity of the slab system to activate diaphragm action.

In essence, the simulation served as a digital prototype, supporting both the analytical characterisation and future experimental validation of the proposed connection concept. It offers a deeper understanding of the structural behaviour associated with precast slab assembly and forms a solid foundation for the refinement of design strategies and performance criteria.

4.3.3. MODELLING ADJUSTMENTS AND CONVERGENCE CHALLENGES

During the development of the finite element simulation in ANSYS, several challenges were encountered, particularly related to convergence under nonlinear conditions. The model was designed to capture realistic interactions between hollow core slabs and the proposed connector, using advanced material properties and complex contact behaviours. However, the solver initially failed to converge, meaning it could not achieve a stable and balanced solution within the specified iteration limits and tolerance thresholds.

In nonlinear finite element analysis, convergence failures can arise due to a combination of factors, including high stress concentrations, incompatible boundary conditions, overly stiff constraints, or excessive strain localisation. In this case, the numerical complexity was intensified by the use of nonlinear concrete behaviour, multiple interacting surfaces, and the detailed geometries of both slabs and connector. This created a challenging environment for achieving a converged solution.

The initial model geometry followed the experimental test configuration, featuring slabs 2000 mm in length. The first strategy employed to resolve the convergence issue involved mesh refinement. The initial 40 mm mesh size was reduced to 30 mm in critical areas around the connector and joint interface. When convergence was still not achieved, the mesh was further refined to 20 mm. Although this finer mesh increased the resolution and provided better strain localisation, it also drastically raised the number of elements and nodes in the model.

At this level of refinement, the simulation exceeded the limitations of the available ANSYS academic licence, which restricts the number of nodes and elements. This resulted in memory overloads and premature termination of the solver, making it impossible to obtain reliable results. It became clear that a compromise between numerical accuracy and computational feasibility was necessary.

To address both convergence difficulties and licensing limitations, a key modelling adjustment was implemented: the slab length was reduced from 2000 mm to 1000 mm. This change preserved the original slab height, width, and reinforcement configuration, while significantly reducing the number of elements required for the simulation. It also improved numerical stability by decreasing cumulative deformation and stress gradients across the length of the model.

This modification means that the numerical simulation represents a scenario where one connector is positioned for every metre along the longitudinal joint between hollow core slabs. While this differs slightly from the full-scale laboratory test, it provides a practical and focused evaluation of the connector’s local shear transfer capacity. This local analysis is particularly relevant for understanding how the connector performs in facilitating diaphragm action without requiring cast-in-place materials.

The final finite element model was meshed with a global element size of 30 mm, which provided an effective balance between resolution and computational efficiency. This mesh size was fine enough to capture local stress concentrations near the connector while remaining within the limitations of the ANSYS academic licence.

The updated model with the reduced slab length and final meshing configuration is shown in Figure 34, which illustrates the simplified geometry adopted to ensure convergence and numerical stability. A detailed view of the structured mesh applied to the slabs and connector region is presented in Figure 35, high5lighting the regular distribution of elements and refinement around critical connection zones.

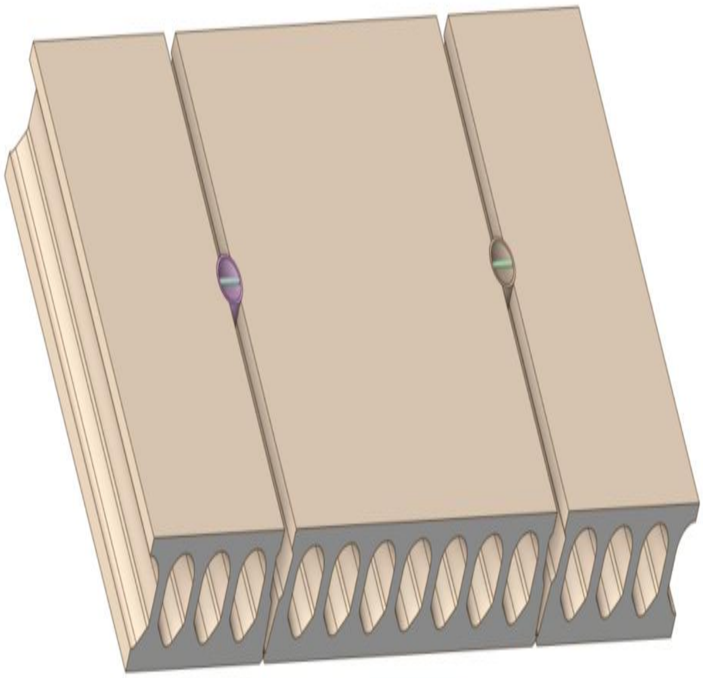

Fig. 34 - Final numerical model configuration with slab length reduced to 1000 mm.

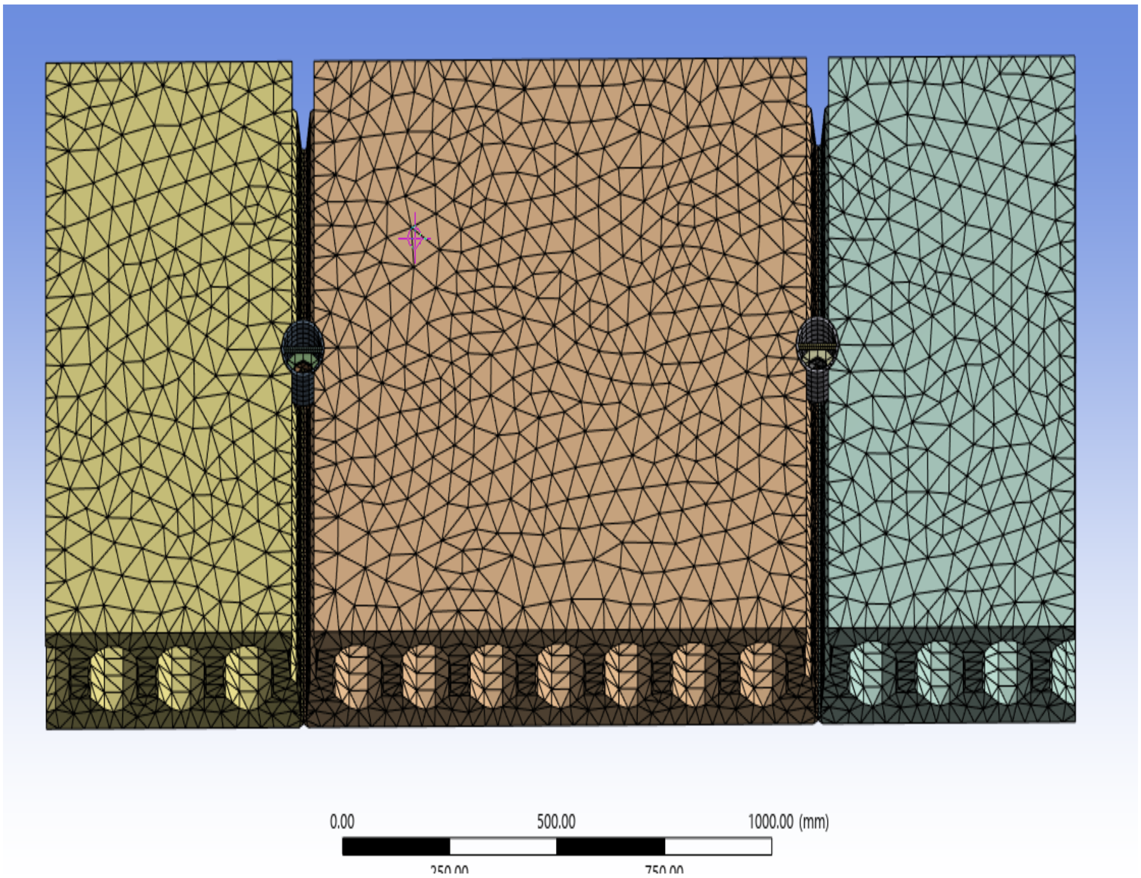

Fig. 35 - Structured mesh applied to the updated model.

In the ANSYS Student edition it was not possible to prescribe a displacement smaller than 1 mm. Although the analysis converged and the resulting displacements, normal stresses and shear stresses were within acceptable limits, the model produced a reaction of roughly 710 kN. This indicates that a force of that magnitude was effectively applied to the central slab, far higher than the value derived from the wind-load design.

To generate results that better match service conditions, the approach was changed. Rather than prescribing a displacement, a force of 12 kN, twice the required design value and well above the 4.8 kNm wind demand (about 6 kN per slab joint), was applied to the central slab. All results discussed in the next section refer to this force-controlled model, which offers a clearer picture of connector behaviour under realistic loading. The supporting calculations and auxiliary data used to establish these load levels are provided in Appendix X.

Through a combination of mesh refinement and geometric simplification, a robust and computationally efficient model was achieved. These adjustments allowed the analysis to remain representative of real-world applications while ensuring the reliability and validity of the numerical outcomes. The implications of these assumptions and their effects on structural performance are further discussed in Chapter 5, where the results of the simulation are evaluated within the broader framework of reversible construction and precast floor systems.

5

DISCUSSION OF RESULTS

5.1. INTRODUCTION

This chapter presents a comprehensive analysis of the numerical results obtained through the finite element simulations performed in ANSYS. Building upon the modelling strategy and parameter definitions outlined in the previous chapters, particular attention is given to the behaviour of the proposed mechanical interlock system under imposed horizontal displacements. The evaluation focuses on the stress distribution in the vicinity of the connector, the transfer of shear forces across slab interfaces, and the extent to which the connector contributes to global diaphragm action.

The results are interpreted with reference to both local and global performance indicators, offering insight into the structural response of the system under quasi-static loading. Graphical outputs and post-processing data are used to illustrate deformation patterns, internal force development, and critical regions of stress concentration. These observations are essential for assessing the feasibility of the connection strategy and verifying whether the expected mechanical behaviour was achieved.

Furthermore, the findings are discussed in light of the practical goals of the connection design, including simplicity, reversibility, and structural efficiency. Where relevant, the results are compared with theoretical expectations or code-based assumptions, enabling a more informed understanding of the connector's potential in real-world applications.

Finally, the chapter concludes by summarising the key outcomes of the study and reflecting on their broader implications. The concluding remarks aim to position the numerical findings within the overall context of the dissertation and suggest possible directions for future experimental and computational research.

5.2. DEFORMATION ANALYSIS

The finite element simulation provided a detailed view of the deformation behaviour of the structure under a horizontal force of 12 kN applied to the central hollow core slab. This load case was selected to represent a critical condition for inter-slab shear transfer and to evaluate the mechanical performance of the proposed connector.

The results revealed that the majority of the structure experienced minimal displacement, with both the connector and the reinforcing bars showing movements of less than 0.007 mm. The concrete displayed slightly higher deformation only in the immediate vicinity of the applied load, where the maximum reached 0.01 mm. These values confirm that the slab system remained essentially rigid under the imposed loading, demonstrating effective global stiffness and negligible in-plane deformation.

The overall deformation of the structure is visualised in Figure 36, which shows the distribution of total displacements using a colour gradient.

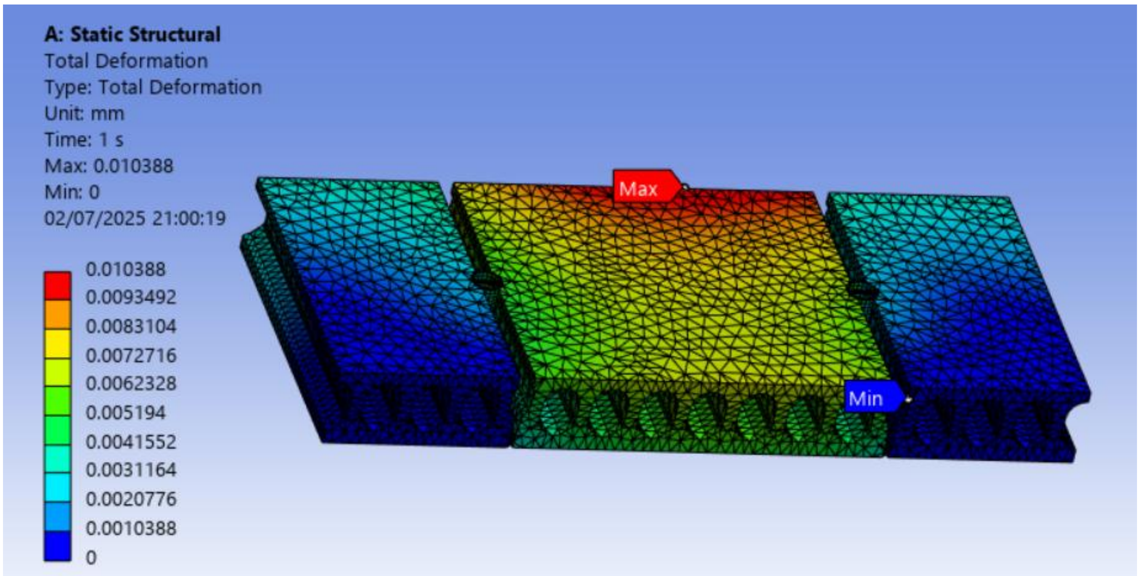

Fig. 36 - Global deformation distribution of the full slab system.

To better understand the connector's performance, a more focused view is presented in Figure 37, showing only the connector and the embedded rebars.

Fig. 37 - Localised deformation in the connector and embedded rebars.

Additionally, Figure 38 illustrates the directional deformation vectors for the connector and rebars. These vectors reveal the primary direction of movement and how the interlock mechanism accommodates shear force through relative displacement between components.

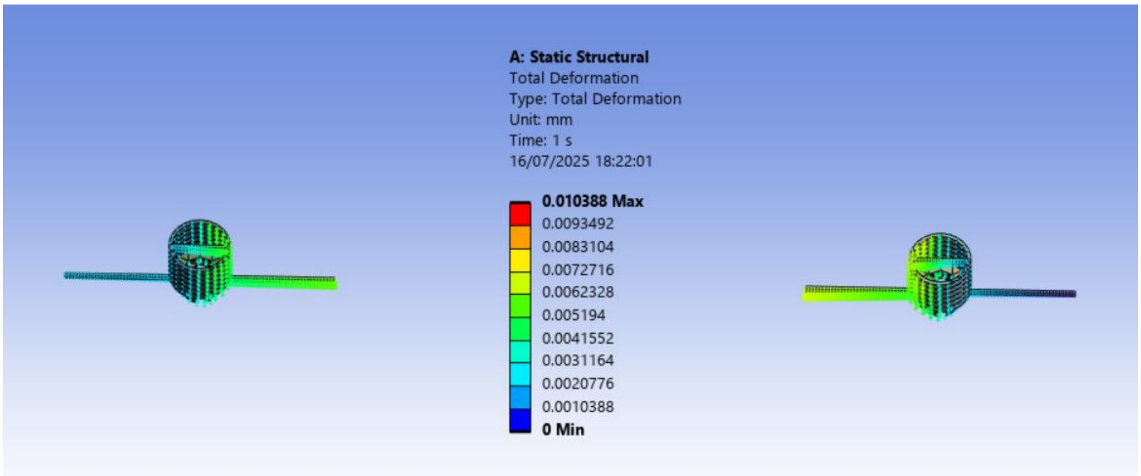

Fig. 38 - Directional deformation vectors in the connector and rebars.

These results collectively indicate that the proposed connector accommodates limited local deformation while preserving the overall structural integrity of the slab system. The observed deformations remain relatively small, with minimal impact on the surrounding concrete.

5.3. EQUIVALENT (VON MISES) STRESS

To complement the deformation analysis presented in the previous section, an evaluation of the internal stress distribution was carried out using the equivalent (Von Mises) stress criterion. This scalar stress measure is widely used in structural and mechanical analysis to estimate the onset of yielding in ductile materials, particularly steel. In the context of this simulation, the Von Mises stress results provide insight into the demand placed on the interlocking connector and its embedded rebars under the imposed horizontal displacement.

The global distribution of equivalent (Von Mises) stresses within the concrete slabs and steel components is illustrated in Figure 39, which presents the full model configuration with a colour scale indicating stress magnitudes. As shown, the vast majority of the concrete volume remains under low stress levels, with values predominantly below 0.50 MPa. This suggests that the structural system is not experiencing significant stress under the imposed lateral force, and that the overall integrity of the concrete body is preserved. These low stress levels are consistent with the limited deformation patterns observed in Section 5.2 and indicate that the applied load does not compromise the structural safety or serviceability of the slab assembly.

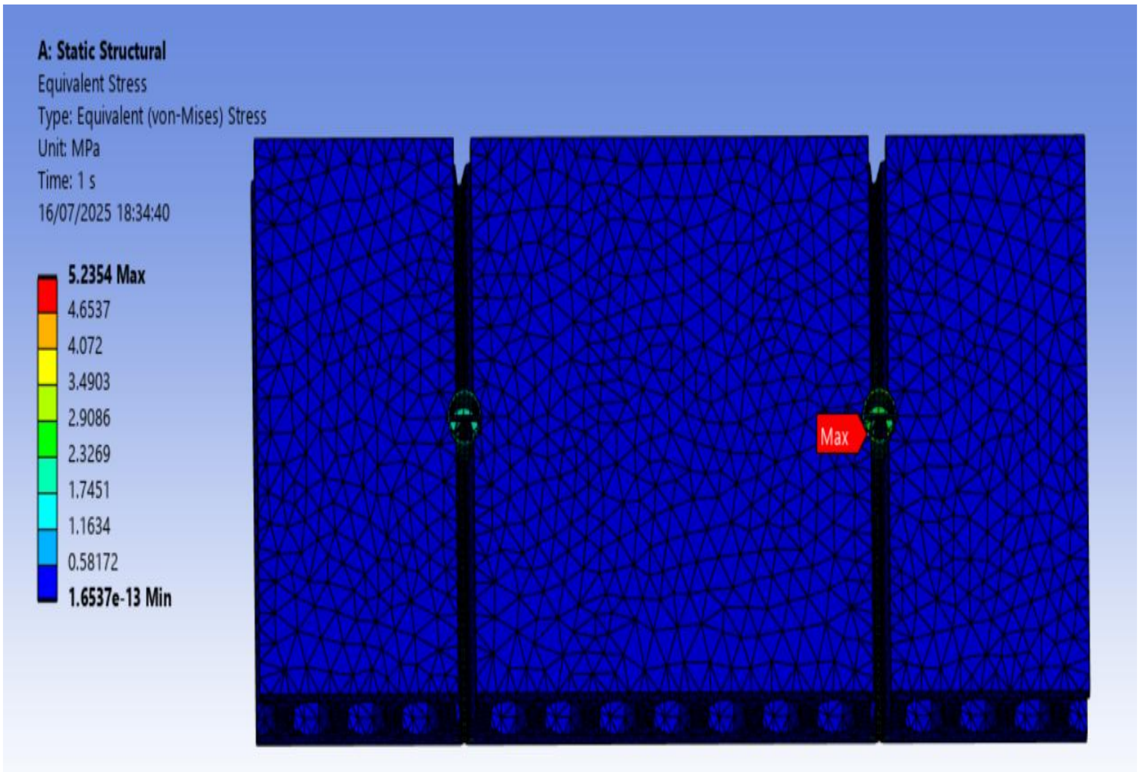

Fig. 39- Global equivalent (Von Mises) stress distribution across the slab system under applied horizontal displacement.

To further verify the stress conditions in the concrete, particularly around the connector region, a capped isosurface visualisation was generated and is presented in Figure 40. In this representation, all regions of the structure experiencing stresses below 3.8 MPa are displayed. This focused representation confirms that even the concrete surrounding the connector, where force transfer is most concentrated, remains within this threshold. Given that the compressive strength of C45/55 concrete is 45 MPa and the average tensile strength is 3.8 Mpa. The analysis therefore reinforces that the connector operates within safe limits, avoiding concrete crushing or cracking in its immediate vicinity.

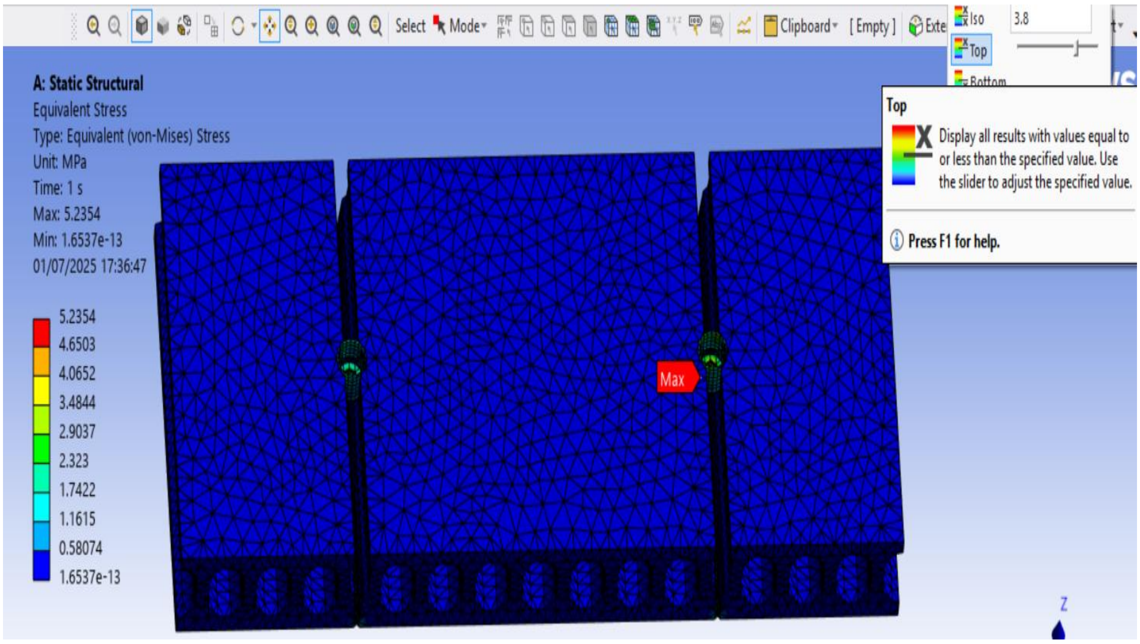

Fig. 40 - Visualisation of the structural system highlighting regions with equivalent stress below 3.8 MPa.

As anticipated, the highest stress concentrations occur within the steel connector and the embedded reinforcement bars, especially in the interlock zone where force transfer is most intense. Figure 41 illustrates this distribution with a colour gradient. The peak stress measured in the connector is 5.24 MPa, far below the yield strength of 400 MPa, corresponding to approximately 80% of the characteristic yield strength (fyk) = 500 MPa. The observed stress is negligible, providing a substantial safety margin for the connector and adjacent rebars.

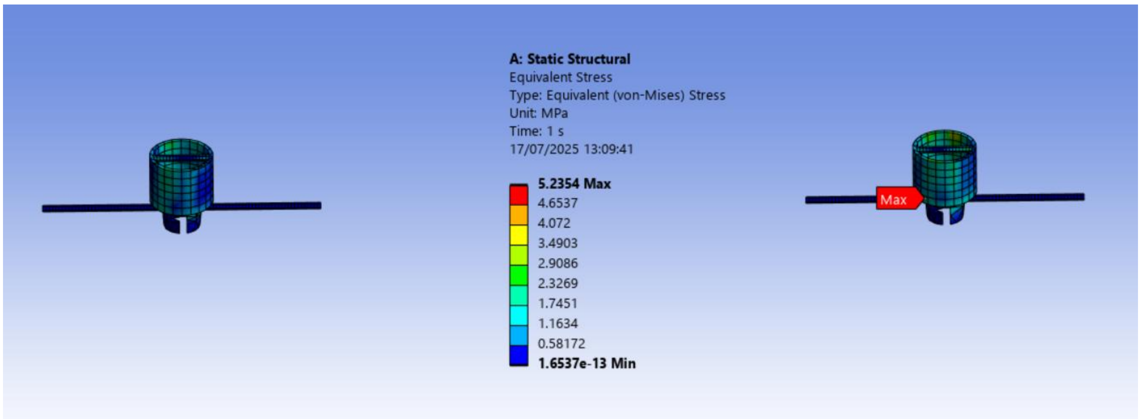

Fig. 41 - View highlighting connectors and rebars' regions with equivalent stress.

A localised peak stress was identified at the interface between the connector and the embedded bar in the central slab, the element to which the horizontal load was applied. Figure 42 presents a close-up of this region. The stress concentration arises from the tight contact between the bar and the edges of the connector's internal slot, yet the low magnitude confirms that the force is effectively distributed over a sufficient surface area.

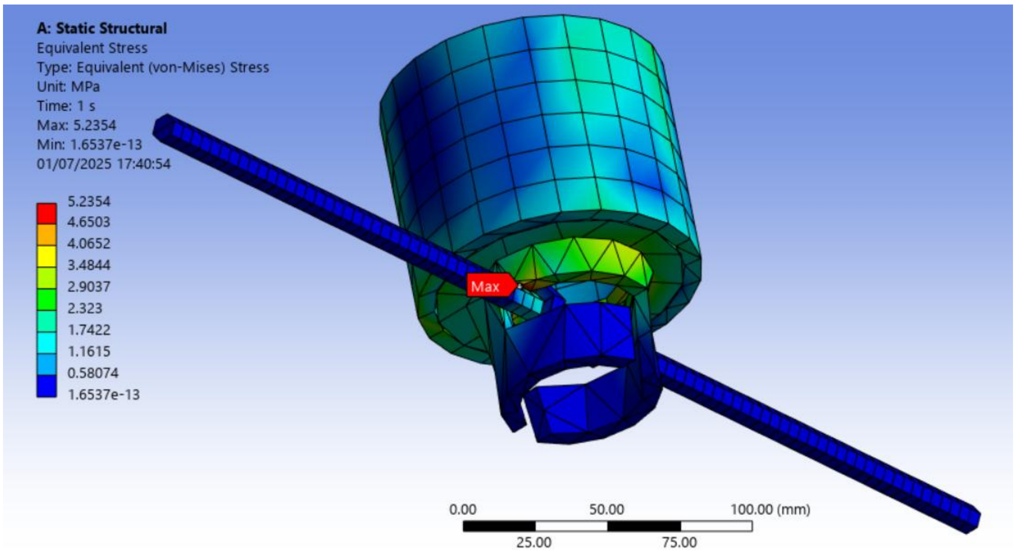

Fig. 42 - Zoomed-in view of the interlock region showing the maximum stress concentration of 5.24 MPa at the rebar–connector interface.

5.4. SHEAR STRESS

One of the key performance criteria for the proposed connector is its capacity to transfer in-plane shear forces between adjacent hollow core slabs, thereby enabling diaphragm action without the use of cast-in-place materials. To evaluate this aspect, the ANSYS simulation was analysed with a focus on shear stress development across the slab-to-slab interface, particularly in the regions surrounding the mechanical connector and the embedded reinforcement.

Figure 43 presents the shear stress distribution along the longitudinal joints and through the connector interface. The results indicate that shear is not uniformly distributed across the contact surface of the slabs, but rather concentrated around the interlock region where the rebars engage mechanically with the connector body. This is a typical behaviour in dry joint configurations, where the absence of bonded materials results in more localised transmission of shear forces.

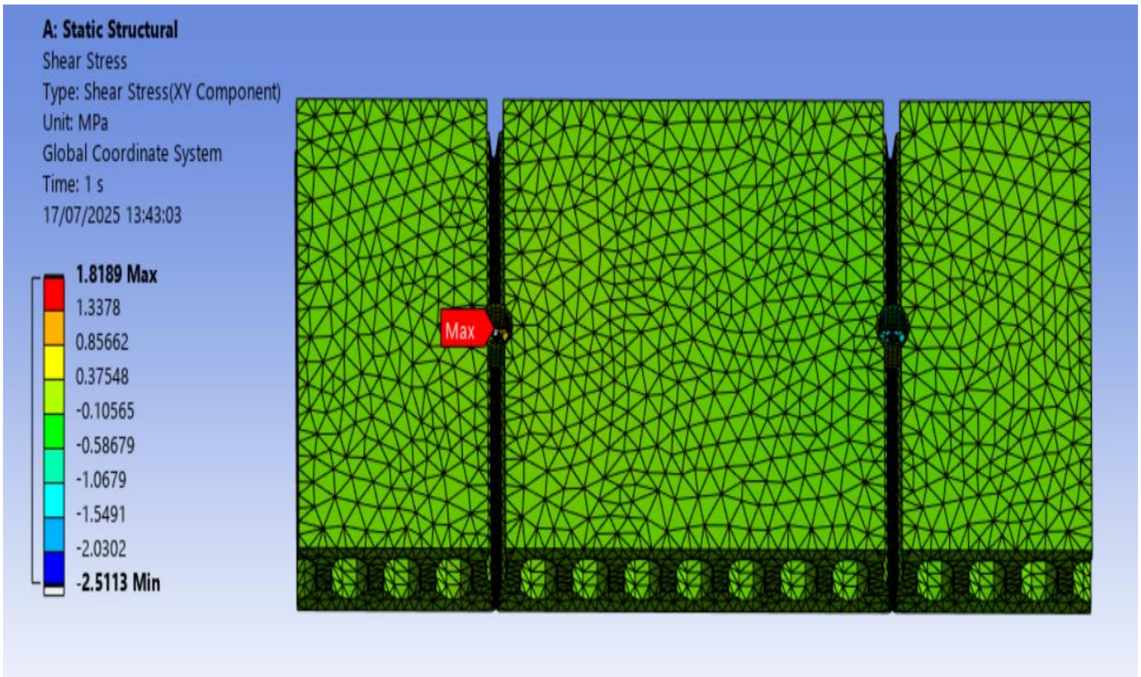

Fig. 43 - Overview of shear stress (SXY) throughout the hollow core slab system.

The stress field in the connector zone highlights the presence of concentrated shear stresses at the transition between the cylindrical shaft and the conical base of the connector. As shown in Figure 44, this area coincides with the geometric discontinuity introduced by the interlock system, where the connector profile changes and the embedded rebars pass through. The concentration of shear in this region suggests it is a critical zone for stress redistribution within the connection system.

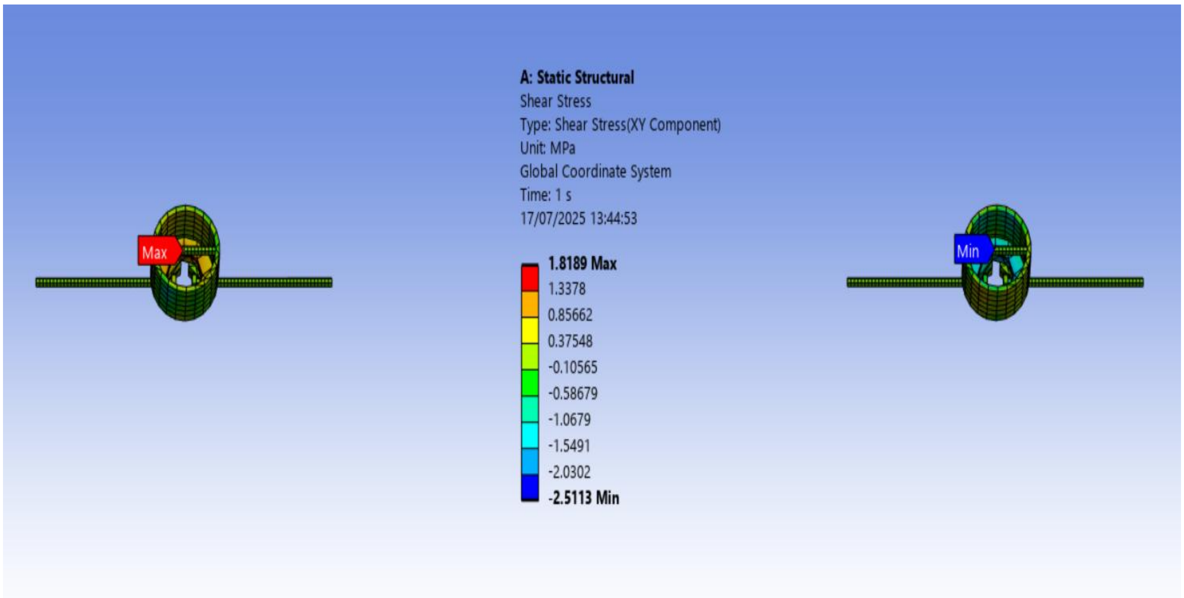

Fig. 44 - Detailed view showing shear stress distribution localised in the connector.

The finite-element analysis revealed that shear stresses are strongly localised in the interlock zone, particularly at the transition between the cylindrical and conical sections of the connector. The peak values are modest:

- Maximum compressive shear stress ≈ 1.82 MPa
- Maximum tensile shear stress ≈ 2.51 MPa

According to Eurocode 3 (EN 1993-1-1), the admissible design stress for S500 steel is 500 MPa, using a partial safety factor $\gamma M0=1.0$. The simulated shear levels are therefore more than two orders of magnitude below the allowable limit, providing an exceptionally large safety margin and confirming that the connector remains well within the elastic range under the applied loading.

Although these results demonstrate that yielding is not a concern, they do not on their own guarantee overall performance; they simply confirm that the stresses are comfortably below critical thresholds.

To offer a broader view of the load path, Table 2 summarises the evolution of shear stress throughout the analysis, listing minimum, maximum and average values at each loading stage. This quantitative record complements the graphical output and underscores the effective transfer of shear through the connector.

Table 2 – Summary of Shear Stress Values During Simulation

Time [s]	Minimum [MPa]	Maximum [MPa]	Average [MPa]
0.2	-0.50225	0.36377	-6.3934e-004
0.4	-1.0045	0.72755	-1.2787e-003
0.6	-1.5068	1.0913	-1.918e-003
0.8	-2.0091	1.4551	-2.5573e-003
1.	-2.5113	1.8189	-3.1966e-003

Note: Values are extracted from integration points within the connector and joint region using equivalent shear stress component SXY.

These numerical results align with the visual analysis and confirm that, even under imposed displacement, the connector remains within the elastic limit under service-level conditions.

5.5. FORCE REACTION

To assess how the joint system redistributes an external load, a horizontal force of 12 kN was applied to the central slab in the x-direction, and the reaction forces at the supports of the two outer slabs were recorded throughout the simulation. Monitoring these reactions reveals how the applied load is transmitted across the connector into the neighbouring units.

Under this force-controlled approach, the supports developed reactions whose principal components act along the x-axis, matching the direction of the applied load.

Figure 45 illustrates the reaction vectors at the supports, confirming that the dominant force component lies in the x-direction, exactly opposite to the applied horizontal force on the central slab.

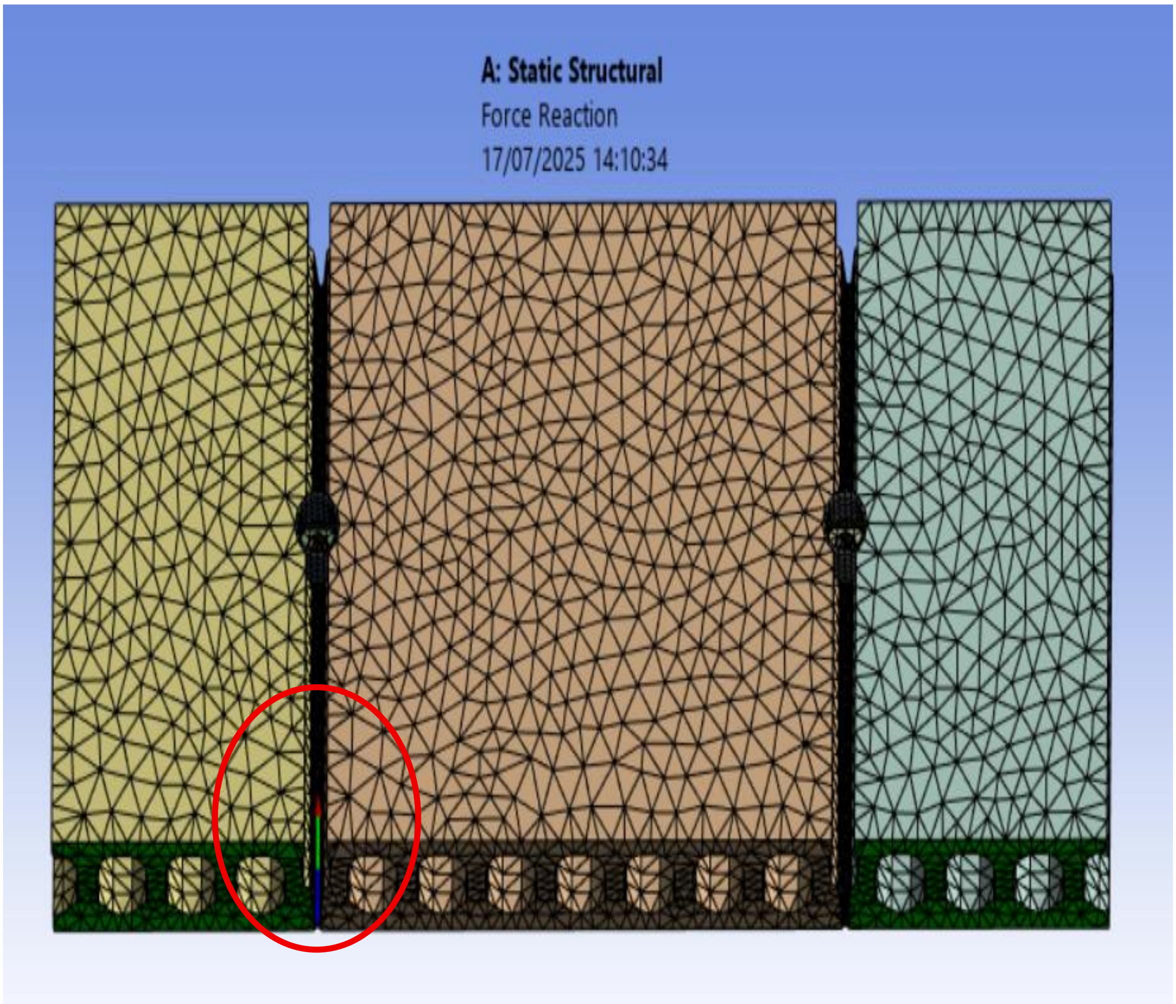

Fig. 45 - Vector representation of support reactions, illustrating the dominant force direction in the x-axis due to imposed horizontal force.

Table 3 lists the numerical values of these reactions at selected analysis steps, detailing the x, y and z components as well as the resultant vector magnitude. The small y and z reactions reflect boundary constraints and second-order effects, whereas the x-component clearly governs the load path, consistent with the objective of evaluating in-plane shear performance.

Table 3 – Force reactions per axis at selected time steps, showing load transfer progression during simulation.

Time [s]	Force Reaction (X) [N]	Force Reaction (Y) [N]	Force Reaction (Z) [N]	Force Reaction (Total) [N]
0.2	-2400.	-0.84595	-6.5941e-005	2400.
0.4	-4800.	-1.6919	-2.6382e-004	4800.
0.6	-7200.	-2.5378	-5.9369e-004	7200.
0.8	-9600.	-3.3837	-1.0555e-003	9600.
1.	-12000	-4.2296	-1.6493e-003	12000

6
CONCLUSION

6.1. SUMMARY OF FINDINGS

The study began with a comprehensive literature review of diaphragm behaviour and circular construction principles, identifying the technical and environmental limitations of conventional connection systems in precast concrete structures. The review highlighted the importance of reversible design and the potential for mechanical connectors to support reuse without compromising structural performance.

Building on these foundations, a novel connector geometry was developed using BIM-based slab data from a widely adopted VBI hollow core slab profile. The connector features a cylindrical top and conical base with internal slots designed to engage embedded reinforcement, forming a mechanical interlock once rotated into position. Operability tests using timber prototypes confirmed the feasibility of this mechanism, particularly when combined with rebars featuring a welded metal “nail head” to prevent slippage and lateral movement.

The connector’s structural behaviour was then evaluated through a detailed ANSYS simulation, designed to replicate a realistic laboratory setup. Due to convergence challenges and computational limitations, modelling adjustments were necessary, including a reduction in slab length from 2000 mm to 1000 mm and refinement of mesh size to 30 mm. It was subjected to a horizontal force of 12 kN, twice the design wind demand of 6 kN per slab joint. These changes enabled a stable numerical environment while maintaining representative loading conditions.

The simulation revealed that:

- Global deformations remained small, with most of the structure displacing less than 0.007 mm under horizontal loading, confirming near-rigid diaphragm behaviour;

- Localised displacement (max. 0.01 mm) occurred primarily at the concrete where the loads were applied;

- Equivalent stress: peak von Mises stress in steel was 5.24 MPa, far below the design yield strength fyd ≈ 435 MPa);

- Concrete stresses throughout the slabs and around the connector stayed well below 3.8 MPa, suggesting no risk of crushing or cracking;

- Shear stress: compressive 1.82 MPa and tensile 2.51 MPa maxima occurred at the cylindrical–conical transition, both comfortably within S500 limits, according to Eurocode 3;

- Load transfer: support reactions balanced the applied load, each outer slab attracting just under 6 kN along the x-axis, with negligible y- and z-components.

6.2. LIMITATIONS

While the numerical model provided valuable insights, some limitations must be acknowledged:

- The reduction in slab length simplified the geometry and may have influenced global behaviour;

- The connector's performance was evaluated under a single load condition and did not account for repeated or dynamic loading;

- The steel-to-concrete interaction, though modelled with nonlinear materials, does not capture all potential real imperfections;

- Experimental validation remains necessary to confirm the numerical predictions and refine the connector's geometry, particularly in areas where high stress concentrations were observed.

6.3. RECOMMENDATIONS FOR FUTURE WORK

Future research should focus on:

- Laboratory testing of the connector in full-scale slab assemblies to validate numerical findings;
- Parametric studies on connector spacing, slab depth and reinforcement detailing to refine design guidance;
- Evaluation of performance under cyclic or seismic loading conditions;
- Integration of the connector into a broader framework of reversible structural systems, including beam-to-slab and wall-to-slab connections;
- Durability assessment of the steel–concrete interface, including corrosion protection and repeated installation cycles;

6.4. FINAL REMARKS

This dissertation explored the development of a demountable mechanical connector for precast hollow core slabs, designed to facilitate diaphragm action without the use of cast-in-place materials. The proposed solution, based on a mechanical interlock system engaging with embedded reinforcement, was examined through operability tests and finite element simulations, contributing to ongoing efforts in designing structurally efficient and reversible precast systems aligned with circular construction principles.

Although definitive conclusions about the connector's structural viability cannot yet be drawn, the results obtained suggest that the system has the potential to perform effectively under service-level conditions. The simulations demonstrated limited local deformation and acceptable stress levels across most components, with the mechanical interlock region emerging as the primary zone of force transfer. These findings, combined with the successful operability of the prototype in dry assembly conditions, provide preliminary indications that the connector concept may yield positive results in real-world applications, particularly in cases where modularity, reusability, and structural continuity are design priorities.

Nonetheless, the limitations inherent to the numerical modelling approach, including simplifications in material behaviour, idealised boundary conditions, and lack of dynamic or long-term loading scenarios, highlight the need for experimental testing to confirm these early insights.

The significance of this research has been recognised through its selection for presentation at the 2nd International Conference on Circularity in the Built Environment (CiBEn), to be held at Tampere University, Finland, from 16 to 18 September 2025. Encouraged by this opportunity, the author intends to continue the development of this work through laboratory-scale testing, with the objective of validating the mechanical performance of the connector and advancing the understanding of its applicability in reversible floor systems. These future steps are expected to provide a stronger foundation for assessing the connector's effectiveness in enabling circularity in precast concrete construction.

BIBLIOGRAPHY

1. Ramsden, D. (2020). *Reducing embodied carbon in construction*. Institution of Civil Engineers, London.

2. ReCreate (2022). *ReCreate – Reuse of precast concrete elements: Design for a circular future*. ReCreate Project (https://recreate-project.eu). Accessed: 4 March 2025.

3. van Vliet, J.C., Durmisevic, E., Brouwers, H.J.H. (2021). *Development of a Demountability Index to Support the Circular Design of Buildings*. Buildings, 1/02/2021, Article 42, MDPI, Basel. https://doi.org/10.3390/buildings11020042

4. Al-Azzawi, A., Turuallo, G., van der Veen, C., Braam, C. (2018). *Investigation of grouted joints for precast concrete deck systems*. Engineering Structures, 15/04/2018, pp. 389–400, Elsevier, Amsterdam.

5. Barbieri, D.M., Mechtcherine, V., Bücker, M., Middendorf, B. (2018). *Durability of dry-joint connections in precast concrete: long-term performance assessment*. Construction and Building Materials, 5/09/2018, pp. 512–520, Elsevier, Amsterdam.

6. Leurini, A., de Domenico, D., Bournas, D.A. (2016). *Modelling diaphragm action in precast floor systems*. Engineering Structures, 10/11/2016, pp. 86–97, Elsevier, Amsterdam.

7. Veenhuis, J. (2024). *Reusability potential of precast hollow-core slabs*. Master's Thesis, TU Delft.

8. CUR (1990). *CUR Recommendation 103: Demountable construction principles*. CUR Committee, Gouda.

9. Durmisevic, E. (2018). *Reversible Building Design – Circularity in Buildings*. Dissertação de Doutoramento, Delft University of Technology.

10. EN 1991-1-4 (2005). *Eurocode 1: Actions on structures – Part 1-4: General actions – Wind actions*. CEN, Brussels.

11. EN 1168+A3 (2011). *Precast concrete products – Hollow core slabs*. CEN, Brussels.

12. ISO 20887 (2020). *Sustainability in buildings and civil engineering works – Design for disassembly and adaptability – Principles, requirements and guidance*. ISO, Geneva.

13. NS 3682 (2022). *Re-use of hollow core slabs – Design, documentation and execution*. Standards Norway, Oslo.

14. CONSOLIS VBI. *Hollow core slab product documentation and BIM files.* Available at: https://vbi.nl. Accessed: 10 March 2025.

APPENDIX A – ANSYS SIMULATION SUMMARY AND MECHANICAL REPORT

A.1. MESH

Table 4 – Mesh information.

Object Name	*Mesh*
State	Solved
Display	
Display Style	Use Geometry Setting
Defaults	
Physics Preference	Mechanical
Element Order	Linear
Element Size	30.0 mm
Sizing	
Use Adaptive Sizing	Yes
Resolution	Default (2)
Mesh Defeaturing	Yes
Defeature Size	Default
Transition	Fast
Span Angle Center	Coarse
Initial Size Seed	Assembly
Bounding Box Diagonal	2608.4 mm
Average Surface Area	52108 mm^2

Minimum Edge Length	5.0 mm
Quality	
Check Mesh Quality	Yes, Errors
Error Limits	Aggressive Mechanical
Target Element Quality	Default (5.e-002)
Smoothing	Medium
Mesh Metric	None
Inflation	
Use Automatic Inflation	None
Inflation Option	Smooth Transition
Transition Ratio	0.272
Maximum Layers	5
Growth Rate	1.2
Inflation Algorithm	Pre
Inflation Element Type	Wedges
View Advanced Options	No
Advanced	
Number of CPUs for Parallel Part Meshing	Program Controlled
Straight Sided Elements	
Rigid Body Behavior	Dimensionally Reduced
Triangle Surface Mesher	Program Controlled

Topology Checking	Yes
Pinch Tolerance	Please Define
Generate Pinch on Refresh	No
Automatic Methods	
Sheet Body Method	Quad Dominant
Sweepable Body Method	Sweep
Statistics	
Nodes	16737
Elements	53452
Show Detailed Statistics	No

A.2. STATIC STRUCTURAL

Table 5 – Analysis.

OBJECT NAME	*STATIC STRUCTURAL (A5)*
STATE	SOLVED
DEFINITION	
PHYSICS TYPE	STRUCTURAL
ANALYSIS TYPE	STATIC STRUCTURAL
SOLVER TARGET	MECHANICAL APDL
OPTIONS	

ENVIRONMENT TEMPERATURE	22. °C
GENERATE INPUT ONLY	NO

Table 6 – Analysis Settings

OBJECT NAME	*ANALYSIS SETTINGS*
STATE	FULLY DEFINED
STEP CONTROLS	
NUMBER OF STEPS	1.
CURRENT STEP NUMBER	1.
STEP END TIME	1. S
AUTO TIME STEPPING	ON
DEFINE BY	SUBSTEPS
INITIAL SUBSTEPS	5.

Minimum Substeps	5.
Maximum Substeps	20.
Solver Controls	
Solver Type	Program Controlled
Weak Springs	Off
Solver Pivot Checking	Program Controlled
Large Deflection	On
Inertia Relief	Off
Quasi-Static Solution	Off
Restart Controls	

Generate Restart Points	Program Controlled
Retain Files After Full Solve	No
Combine Restart Files	Program Controlled
Nonlinear Controls	
Force Convergence	Program Controlled
Moment Convergence	Program Controlled
Displacement Convergence	Program Controlled
Rotation Convergence	Program Controlled

Line Search	Program Controlled
Advanced	
Inverse Option	No
Contact Split (DMP)	Program Controlled
Output Controls	
Output Selection	None
Stress	Yes
Back Stress	No
Strain	Yes
Contact Data	Yes
Nonlinear Data	No
Nodal Forc	No

ES	
VOLUME AND ENERGY	YES
EULER ANGLES	YES
GENERAL MISCELLANEOUS	NO
CONTACT MISCELLANEOUS	NO
STORE RESULTS AT	ALL TIME POINTS
RESULT FILE COMPRESSION	PROGRAM CONTROLLED
ANALYSIS DATA MANAGEMENT	
SOLVER FILES DIRECTORY	C:\USERS\RAPHA\ONEDRIVE\DESKTOP\PROJECT_TESE\ANSYS_GEOMETRY_FORCE_1M_2C_10MM_FILES\DP0\SYS\MECH\

Future Analysis	None
Scratch Solver Files Directory	
Save MAPDL db	No
Contact Summary	Program Controlled
Delete Unneeded Files	Yes
Nonlinear Solution	Yes
Solver Units	Active System
Solver Unit System	nmm

Table 7 – Loads.

Object Name	*Fixed Support*	*Pressure*	*Pressure 2*	*Force*
State	Fully Defined			
Scope				
Scoping Method	Geometry Selection			
Geometry	2 Faces			1 Face
Definition				
Type	Fixed Support	Pressure		Force
Suppressed	No			
Define By		Normal To		Vector
Applied By		Surface Effect		
Loaded Area		Deformed		
Magnitude		1.25e-002 MPa (ramped)		-12000 N (ramped)
Direction				Defined

A.3. SOLUTION

Table 8 – Solution

Object Name	***Solution (A6)***
State	**Solved**
Adaptive Mesh Refinement	
Max Refinement Loops	**1.**
Refinement Depth	**2.**
Information	
Status	**Done**
MAPDL Elapsed Time	**54. s**
MAPDL Memory Used	**353. MB**

MAPDL Result File Size	162.31 MB
Post Processing	
Beam Section Results	Yes
On Demand Stress/Strain	No

Table 9 – Solution Information

Object Name	*Solution Information*
State	Solved
Solution Information	
Solution Output	Solver Output
Newton-Raphson Residuals	0
Identify Element Violations	0
Update Interval	2.5 s
Display Points	All
FE Connection Visibility	
Activate Visibility	Yes
Display	All FE Connectors
Draw Connections Attached To	All Nodes
Line Color	Connection Type
Visible on Results	No
Line Thickness	Single
Display Type	Lines

Table 10 – Solution Information (Results)

Object Name	*Equivalent Stress*	*Total Deformation*
State	Solved	
Scope		
Scoping Method	Geometry Selection	
Geometry	All Bodies	
Definition		
Type	Equivalent (von-Mises) Stress	Total Deformation
By	Time	
Display Time	Last	
Separate Data by Entity	No	
Suppressed	No	
Integration Point Results		
Display Option	Averaged	
Average Across Bodies	No	
Results		
Minimum	1.6537e-013 MPa	0. mm
Maximum	5.2354 MPa	1.0388e-002 mm
Average	0.17358 MPa	3.7834e-003 mm
Minimum Occurs On	Component1\Sólido	
Maximum Occurs On	Component1\Sólido	

Information	
Time	1. s
Load Step	1
Substep	5
Iteration Number	7

Table 11 – Solution Information (Results Charts)

Object Name	*Stiffness Energy*	*Kinetic Energy*
State	Solved	
Definition		
Type	Stiffness Energy	Kinetic Energy
Suppressed	No	
Results		
Minimum	1.503 mJ	7.8886e-031 mJ
Maximum	37.577 mJ	7.8886e-031 mJ

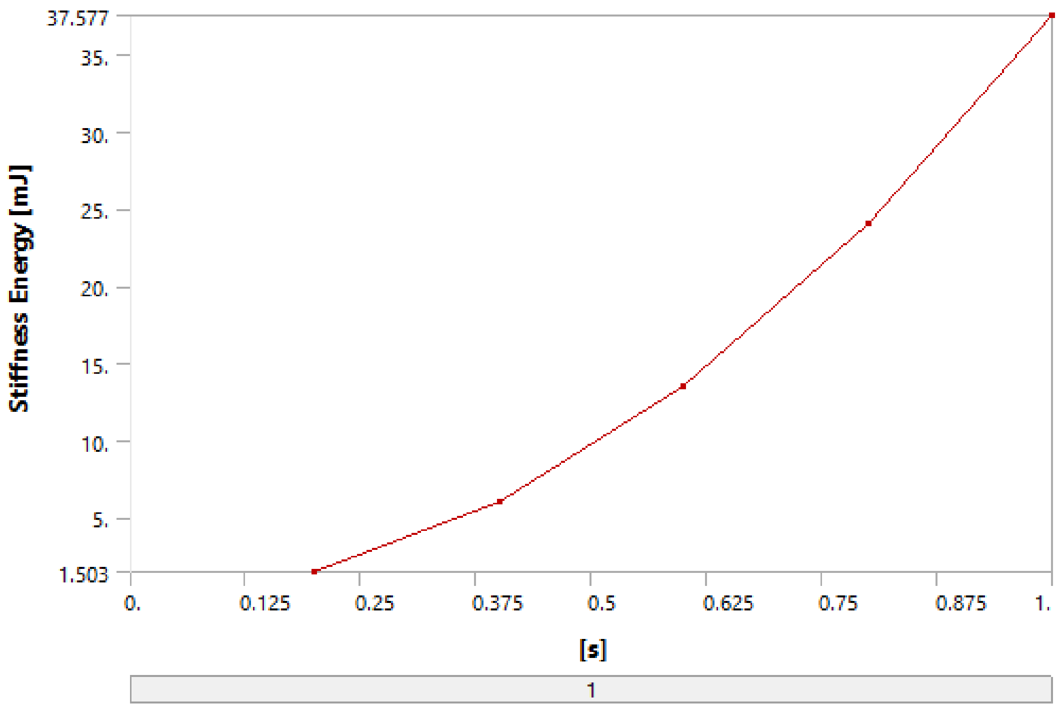

Fig. 46 - Solution Information (Stiffness Energy).

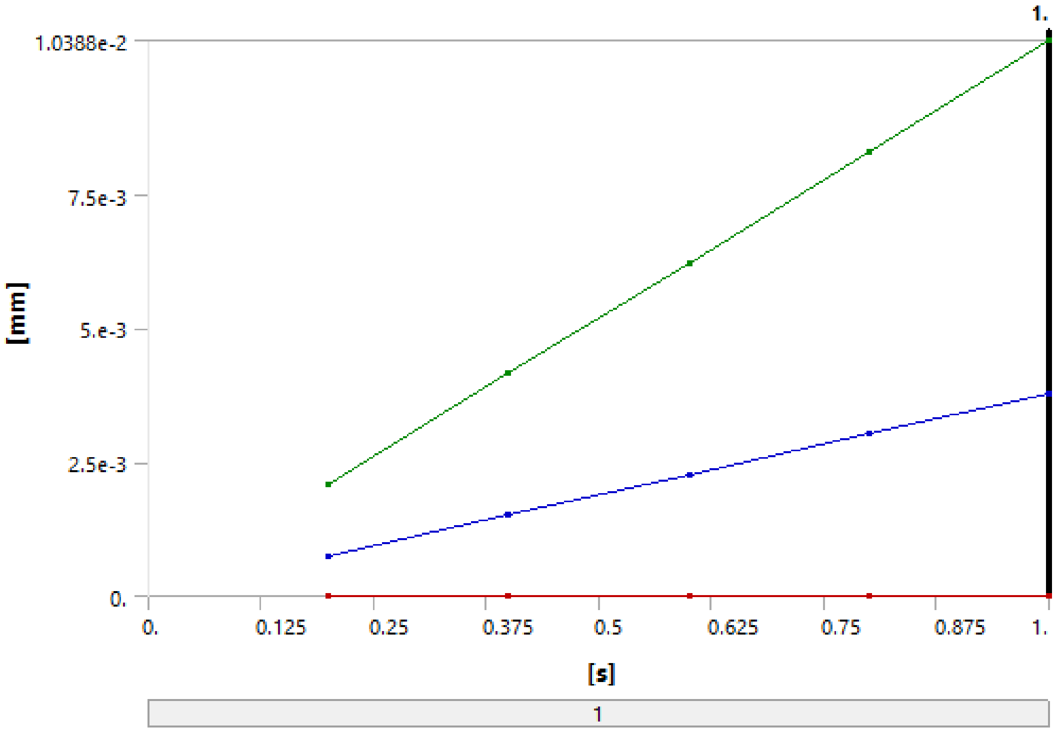

Fig. 47 – Total deformation (mm).

Table 12 – Total Deformation

Time [s]	Minimum [mm]	Maximum [mm]	Average [mm]
0.2	0.	2.0774e-003	7.5664e-004
0.4		4.155e-003	1.5133e-003
0.6		6.2325e-003	2.27e-003
0.8		8.3102e-003	3.0267e-003
1.		1.0388e-002	3.7834e-003

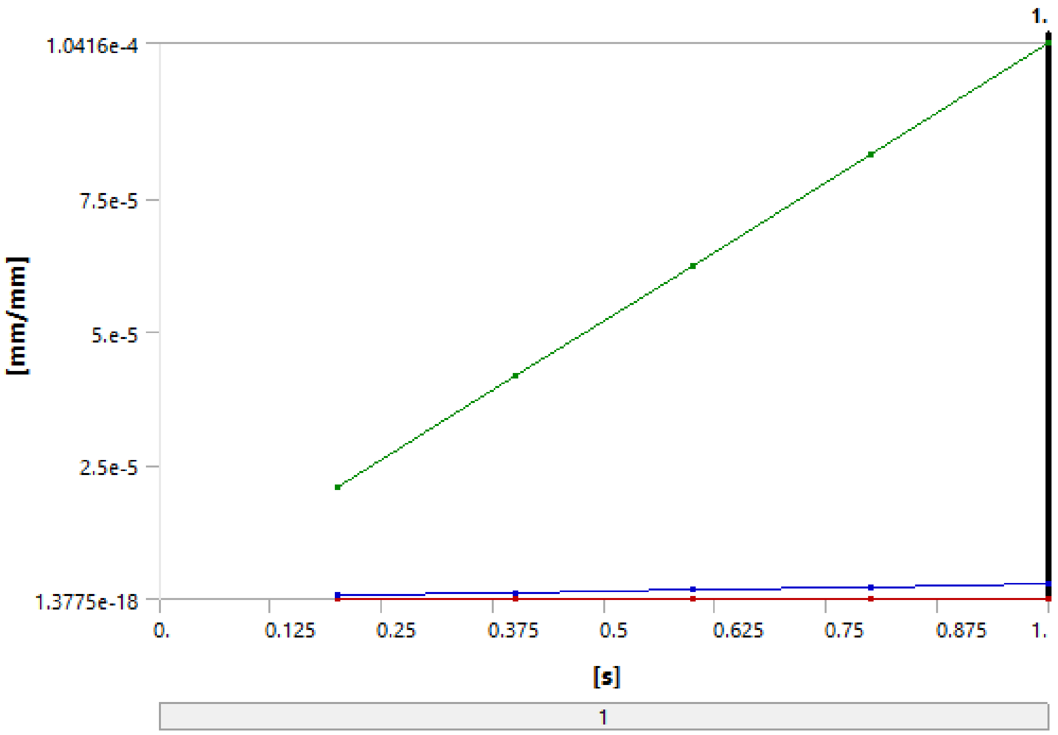

Fig. 48 – Equivalent Total Strain (mm/mm).

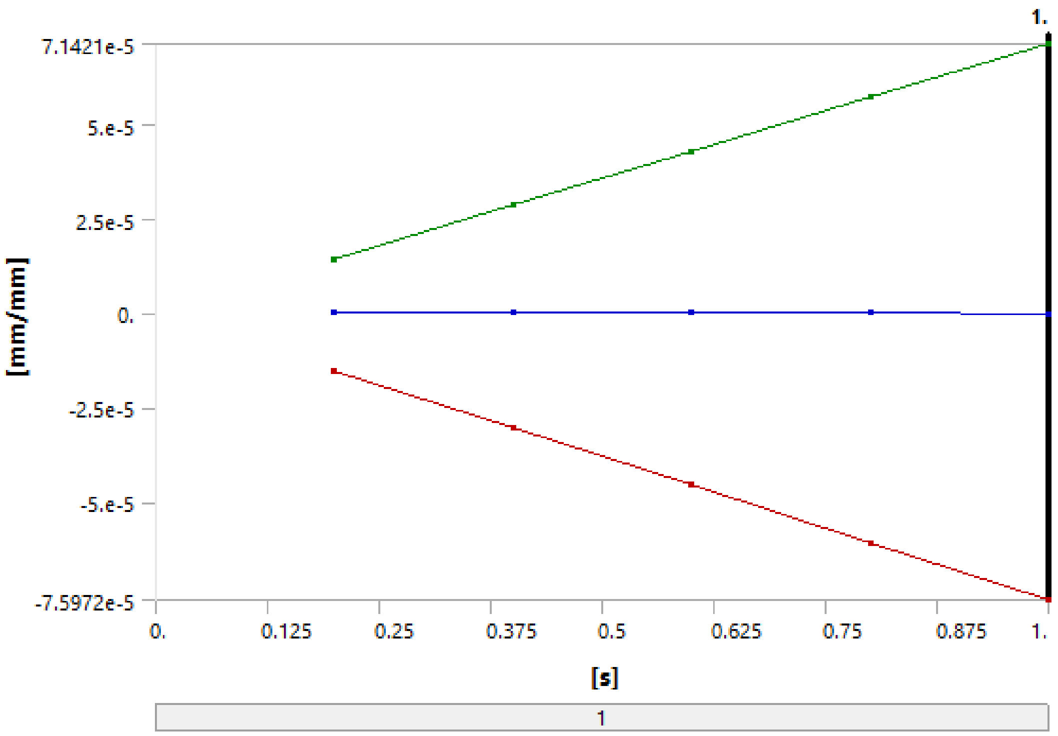

Fig. 49 – Shear Elastic Strain (mm/mm).

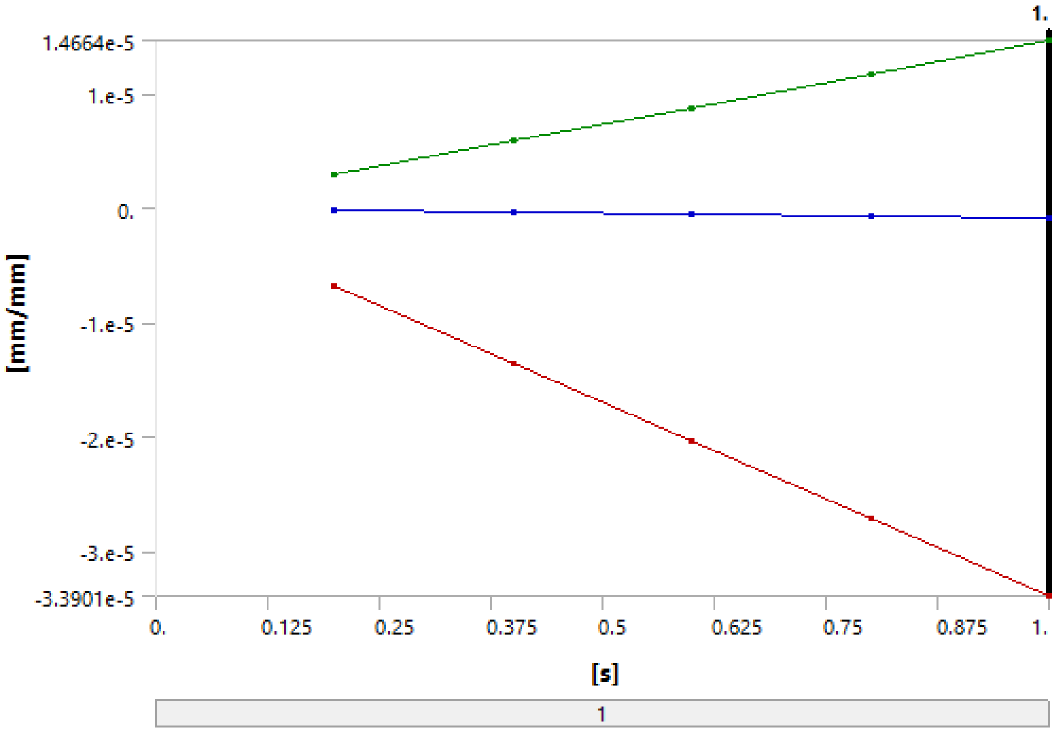

Fig. 50 – Normal Elastic Strain (mm/mm).

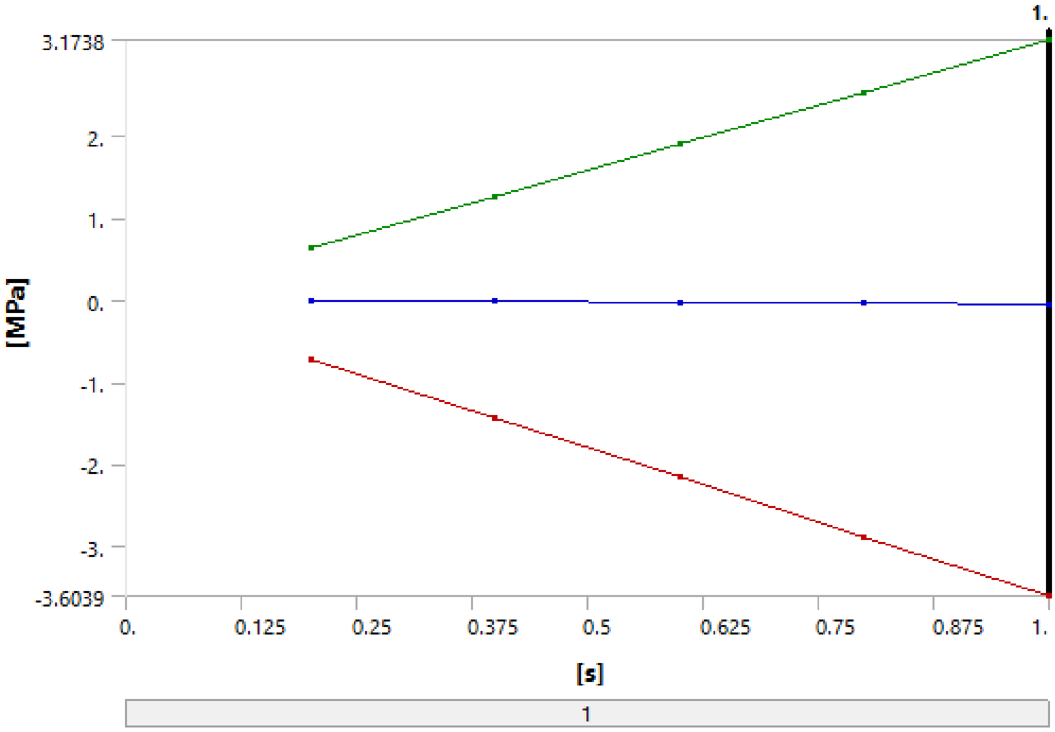

Fig. 51 – Normal Stress (MPa).

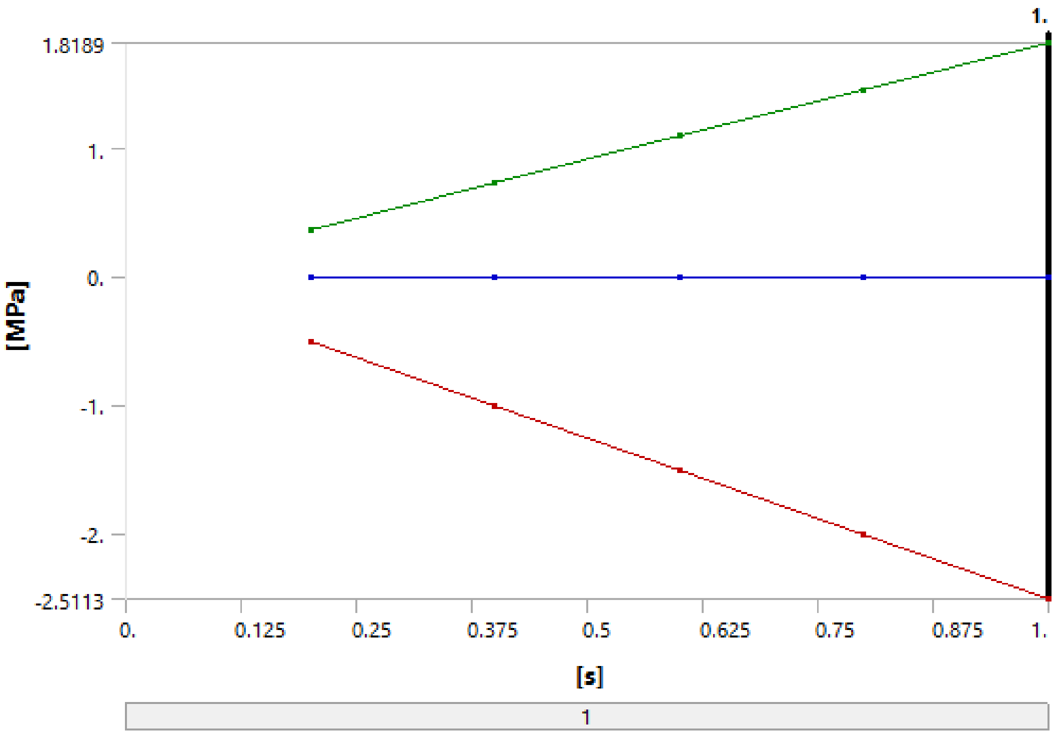

Fig. 52 – Shear Stress (MPa).

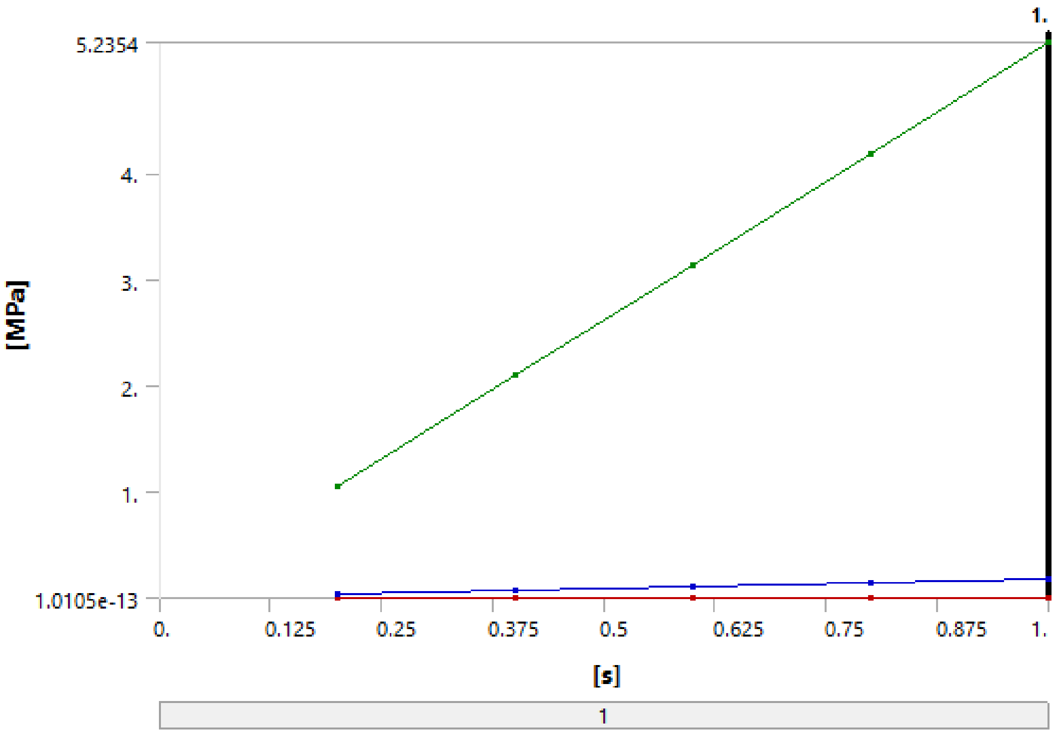

Fig. 53 – Equivalent Stress (MPa).

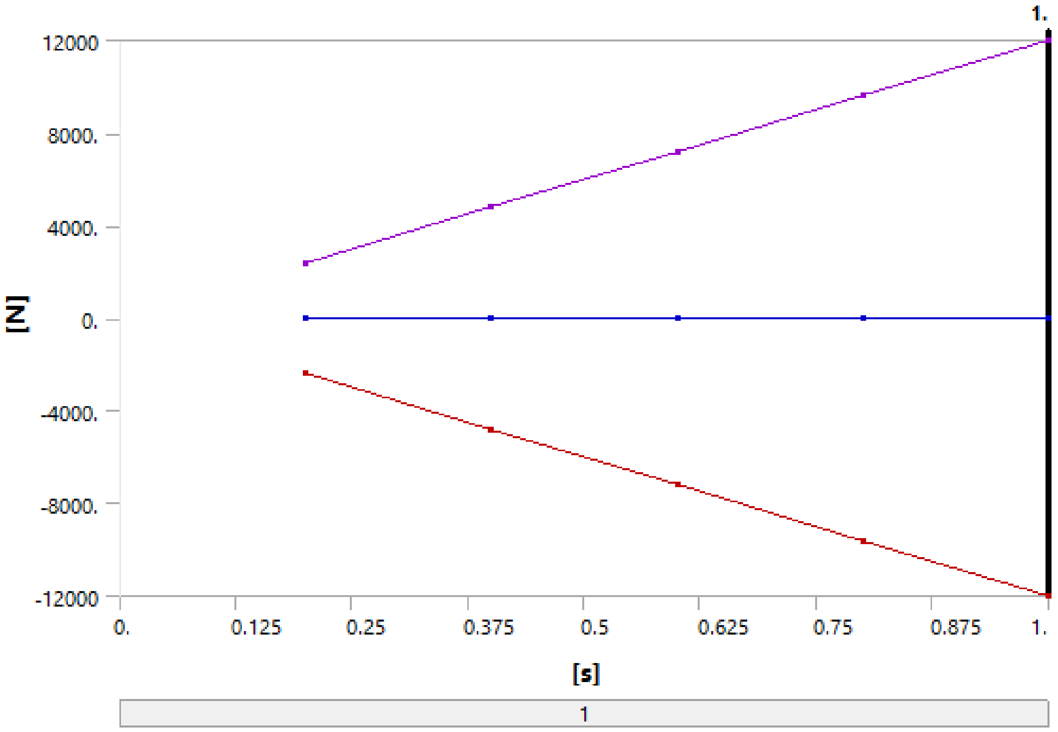

Fig. 54 – Force Reaction (N).

Table 13 – Force Reaction

Time [s]	Force Reaction (X) [N]	Force Reaction (Y) [N]	Force Reaction (Z) [N]	Force Reaction (Total) [N]
0.2	-2400.	-0.84595	-6.5941e-005	2400.
0.4	-4800.	-1.6919	-2.6382e-004	4800.
0.6	-7200.	-2.5378	-5.9369e-004	7200.
0.8	-9600.	-3.3837	-1.0555e-003	9600.
1.	-12000	-4.2296	-1.6493e-003	12000